SOVIET PHYSICS

USPEKHI

A Translation of Uspekhi Fizicheskikh Nauk

SOVIET PHYSICS USPEKHI (Russian Vol. 85, Nos. 1 and 2) JULY-AUGUST, 1965

621.378.1

MULTIPHOTON PROCESSES

A. M. BONCH-BRUEVICH and V. A. KHODOVOĬ

Usp. Fiz. Nauk 85, 3-64 (January, 1965)

CONTENTS

I. ELEMENTARY THEORY AND GENERAL REVIEW OF EXPERIMENTS ON MULTIPHOTON PROCESSES

1. Introduction

A multiphoton process is defined here as interaction between radiation and matter, accompanied by absorption or emission (or both) of not less than two photons per elementary act. The probability of such an elementary act cannot be formally represented in the form of a product of the probabilities of absorption and emission of individual photons.

Interest in multiphoton processes has increased strongly in recent years in connection with the observation of quantum phenomena in the radio band, on the one hand, and the appearance of optical quantum generators (lasers) on the other.

Although multiphoton processes were considered theoretically even during the first years of development of quantum mechanics[1-3], the experimental techniques of that time did not make it possible to observe many of the predicted phenomena. The main difficulty in the study of multiphoton processes is their exceedingly low probability, compared with single-photon processes. As a rule, in order to observe multiphoton processes it is necessary to have radiation densities that are many orders of magnitude larger than those used for the observation of single-photon processes. In the optical band, prior to the appearance of lasers, only two-photon processes of light scattering could be observed experimentally (resonant fluorescence or Rayleigh and Raman scattering). Multiphoton processes connected with the absorption or induced emission of several photons of the radiation exciting the field per elementary act were first observed in the radio band in connection with the relative simplicity of constructing sufficiently powerful radiation sources in this band, and then in connection with the appearance of lasers in the optical band.

The purpose of the present review is to describe briefly the main ideas connected with the investigations of multiphoton processes, and the main results of the experimental and theoretical investigations. In Chapter I we consider the elementary theory of multiphoton processes and present a general review of the experiments. In the discussion of the results of the most interesting experimental research on multiphoton processes (Chapters II and III), we have confined ourselves to only the main ideas and trends of research in this field, occurring during the last decade. The review includes articles published through July 1964.

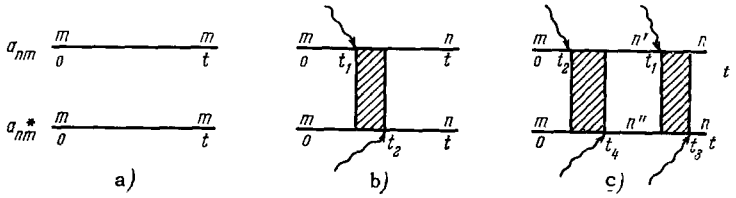

FIG. 1. Diagram representation of the terms of the perturbation theory series for the state amplitudes a_{nm}.

2. Elementary Theory of Multiphoton Processes

1. Fundamental relations. Multiphoton processes are described by second and higher approximations of perturbation theory for the interaction between the radiation field and matter. We consider a quantum system* described by a time-independent Hamiltonian $\hat{H}_0$, under the influence of a perturbation whose operator $\hat{V}(t)$ is of the form

$$V(t)=\begin{cases} V(t), & \text{if} \quad 0\leqslant t\leqslant\tau, \\ 0, & \text{if} \quad t<0,\ t>\tau \end{cases} \tag{1}$$

(we shall henceforth take the perturbation to mean the action of the radiation field, say, on the atom). The behavior of such a system is described by a Schrödinger equation

$$i\hbar\frac{\partial\psi}{\partial t}=(\hat{H}_0+\hat{V}(t))\,\psi, \tag{2}$$

which has no stationary solution. The integral (2) is best sought in the form

$$\psi=\sum_n a_n(t)\,\Phi_n\exp\left(-\frac{iE_nt}{\hbar}\right), \tag{3}$$

where E_n and Φ_n are respectively the eigenvalues and the eigenfunctions of the operator $\hat{H}_0$. We assume that at the instant t = 0 the system is in a stationary state with energy E_m, that is

$$a_n(t)=\delta_{nm},\quad \text{when } t\leqslant 0.$$

After termination of the action of the perturbation, the coefficients $a_n(t)$ assume new constant values $a_{nm}(\tau)$, which depend on the form of the perturbation and on the initial state (designated by the second subscript), that is, when $t\geq\tau$ we have

$$\psi_{\text{fin}}=\sum a_{nm}(\tau)\,\Phi_n\exp\left(-\frac{iE_nt}{\hbar}\right). \tag{4}$$

The square of the modulus of the coefficient $a_{nm}(\tau)$ is

$$W_{mn}(\tau)=|a_{nm}(\tau)|^2 \tag{5}$$

and represents the probability that the system will be situated in a certain stationary state with energy E_n, that is, the probability of the system going over, within a time τ and under the influence of the perturbation, from the initial state m into the state n.

In the solution of many problems in quantum mechanics, it is sufficient to confine oneself to a calculation of the moduli of the coefficients a_{nm}. However, for a detailed description of the system it is necessary to know the complete wave function, so that the phases of the coefficients a_{nm} must also be taken into account.*

If the perturbation is not too large and the coefficients $a_n(\tau)$ change little after a time τ relative to their initial values, then the a_{nm} can be obtained by successive approximations and represented in the form of an infinite series[4]

$$\begin{aligned} a_{nm}(t)&=a_{nm}^{(0)}+a_{nm}^{(1)}+a_{nm}^{(2)}+a_{nm}^{(3)}+\ldots \\ &=\delta_{nm}+(i\hbar)^{-1}\int_0^t V_{nm}(t_1)\,e^{i\omega_{nm}t_1}\,dt_1 \\ &+\sum_{n'}(i\hbar)^{-2}\int_0^t V_{nn'}(t_1)\,e^{i\omega_{nn'}t_1}\,dt_1\int_0^{t_1}V_{n'm}(t_2)\exp(i\omega_{n'm}t_2)\,dt_2 \\ &+\sum_{n',\,n''}(i\hbar)^{-3}\int_0^t V_{nn'}(t_1)\exp(i\omega_{nn'}t_1)\,dt_1\int_0^{t_1}V_{n'n''}(t_2) \\ &\times\exp(i\omega_{n'n''}t_2)\,dt_2\int_0^{t_2}V_{n''m}(t_3)\exp(i\omega_{n''m}t_3)\,dt_3+\ldots \end{aligned} \tag{6}$$

Here $V_{ab}(t)$—matrix element of the operator $\hat{V}(t)$ between the states a and b, and $\hbar\omega_{ab}=E_a-E_b$.

It will be useful in the future to consider some diagram representations which illustrate the meaning of each term of this series[5,6]. In the zeroth approximation $a_{nm}(t)=a_{nm}^{(0)}=\delta_{nm}$ and $a_{nm}^*(t)=a_{nm}^{(0)*}=\delta_{nm}$, which can be represented in the form of the diagram of Fig. 1a, on which the index above the time axis indicates the state for which a_{nm} and a_{nm}^* differ respectively from zero. In the zeroth approximation, for all t we have only $a_{nm}=a_{mm}$ and $a_{nm}^*=a_{mm}^*$, and consequently only $|a_{mm}|^2$, different from zero, that is, the atom remains all the time in the initial state (the zeroth approximation does not take into account the perturbations).

In the first approximation

$$a_{nm}(t)=a_{nm}^{(1)}(t)=(i\hbar)^{-1}\int_0^t V_{nm}(t_1)\exp(i\omega_{nm}t_1)\,dt_1$$

and

$$a_{nm}^*(t)=a_{nm}^{(1)*}(t)=(-i\hbar)^{-1}\int_0^t V_{nm}^*(t_2)\exp(-i\omega_{nm}t_2)\,dt_2,$$

which is represented by the diagram of Fig. 1b. This diagram shows that the coefficient a_{nm} differs from zero in the interval from t_1 to t, while a_{nm}^*--in the interval from t_2 to t. Inasmuch as t_1 and t_2 are simply

*For concreteness we shall henceforth take the quantum system to mean an atom.

*Phenomena which require an account of the phase relations between the coefficients a_{nm} will be considered in Chapter III.

integration variables and therefore are the running coordinates on the diagram of Fig. 1b, there are no grounds for assuming beforehand that $t_1 = t_2$. At the same time, were we to have $t_1 = t_2$, then for $t < t_1$ only the $a^{(0)}_{mm}$ and $a^{(0)*}_{mm}$ would differ from zero (that is, only $|a^{(0)}_{mm}|^2$ would be different from zero), and the system could be observed only in the initial state m. In exactly the same manner, we would have for $t > t_1$ only $|a^{(1)}_{nn}|^2 \neq 0$, and the system is in the state n. Thus, the instant of time $t_1 = t_2$ comes into play in this case as the instant when the quantum system goes over from the state m into the state n under the influence of the perturbation. If $t_1 \neq t_2$, then in the interval $t_2 > t > t_1$ the nonvanishing coefficients are $a^{(0)}_{mm}$ and $a^{(1)*}_{nm}$ or $a^{(1)}_{nm}$ and $a^{(0)*}_{mm}$, that is, the system can be in a superposition state. Getting ahead of ourselves, we note that the magnitude of the time interval $t_2 - t_1$ depends essentially on the spectrum of the perturbation and plays the role of the duration of the elementary act of the single-photon transition.

In the second approximation

$$a_n(t) = a^{(2)}_{nm}(t) = \sum_{n'} (i\hbar)^{-2} \int_0^t V_{nn'}(t_1) \exp(i\omega_{nn'}t_1)\, dt_1 \times \int_0^{t_1} V_{n'm}(t_2) \exp(i\omega_{n'm}t_2)\, dt_2$$

and

$$a^*_n(t) = a^{(2)*}_{nm}(t) = \sum_{n''} (i\hbar)^{-2} \int_0^t V^*_{nn''}(t_3) \times \exp(-i\omega_{nn''}t_3)\, dt_3 \int_0^{t_3} V_{n''m}(t_4) \exp(-i\omega_{n''m}t_4)\, dt_4,$$

which is represented by the corresponding diagram on Fig. 1c. Now, in the time interval from 0 to t, the nonzero amplitudes are those of the intermediate (n′, n″) and final (n) states. Summation over the intermediate states reflects the possibility of attaining the final state via a series of intermediate states, which are connected with the initial and final states by nonzero matrix elements. In each transition, the system absorbs (or emits) one photon. Consequently the transition $m \rightarrow n$ corresponds to a two-photon process.

If $t_2 = t_4$ and $t_1 = t_3$, then for $t < t_2$ only $|a^{(0)}_{mm}|^2 \neq 0$ and the system would be in a state m; for $t_2 < t < t_1$ the system can be either in pure intermediate states n′ or n″ ($|a^{(1)}_{n'm}|^2 \neq 0$ or $|a^{(1)}_{n''m}|^2 \neq 0$), as well as in their superposition state; finally, when $t > t_1$ the system is in state n. Thus, the second approximation regards the transition $m \rightarrow n$ as going in two stages through a series of intermediate states. In the general case $t_2 \neq t_4$ and $t_1 \neq t_3$; the time intervals $t_4 - t_2$ and $t_3 - t_1$ then play the role of transition times from the initial into the intermediate and from the intermediate into the final state, and the gap between these intervals is the time between individual transitions in the two-photon process.

In analogous fashion we can regard the third and higher approximations, which describe processes in which three and more photons participate in each transition from the initial to the final state.

2. Some characteristics of the single-photon processes. We shall review, using as an example the single-photon processes, some important concepts which will be extensively used in what follows. By way of an example let us consider in the dipole electric approximation a single-photon process of transition of an atom from the lower state m to the upper state n under the influence of the radiation field. This field will be regarded classically, for the sake of simplicity.* Then

$$V(t) = -\mathbf{d}\mathbf{E}(t), \tag{7}$$

where d—atomic dipole moment operator and E(t)—electric field intensity at the point of the location of the atom. The probability of the transition $m \rightarrow n$ within a time τ, is, in accordance with (5) and (6)

$$W_{mn}(\tau) = |a^{(1)}_{nm}(\tau)|^2 = \int_0^\tau dt_1 \times \int_0^\tau E^*(t_1) E(t_2) \exp[-i\omega_{nm}(t_1 - t_2)]\, |d_{mn}|^2 \hbar^{-2}\, dt_2, \tag{8}$$

where d_{mn}—matrix element of the projection of the dipole moment on the direction of the field E(t). In the radio-frequency band, the field can be described by an analytic function, and in the simplest case by a harmonic function. In the optical band, the fields E(t) are aggregates of a large number of fields of individual harmonics with random phases[8] (we are disregarding for the time being the case of optical quantum generators). As a result, the amplitude and the phase of the field are subject to irregular fluctuations, the speed of which depends essentially on the width $\Delta\omega$ of the spectral band E(t), and may be regarded as invariant only in the time interval $\Delta t \lesssim (\Delta\omega)^{-1}$. For such fields, the probability of the transition $m \rightarrow n$ is calculated by averaging $W_{mn}(\tau)$ over the distribution W(E) of the field E(t)[9]:

$$\overline{W}_{mn}(\tau) = \sum_{E(t)} W_{mn}(\tau, E) W(E), \tag{9}$$

where $W_{mn}(\tau, E)$—probability of the $m \rightarrow n$ transition for a definite field E(t). This averaging is a linear operation and reduces to averaging the product $E^*(t_1)E(t_2)$ under the integral sign in (8). The result of the averaging $\langle E^*(t_1)E(t_2)\rangle$ is the second moment or the correlation function $\Phi(t_1, t_2)$ of the field E(t), knowledge of which is sufficient for the calculation of the average probability $\overline{W}_{mn}(\tau)$. In the case of the usual optical sources of radiation, with constant intensity, the correlation function depends only on the time

*A quantum-theoretical consideration of the radiation field does not change the results[7].

difference $t_1 - t_2$, and is connected with the spectral density $I(\omega)$ in the following fashion[8,10,11]:

$$\Phi(t_1, t_2) = \Phi(t_1 - t_2) = 8\pi c^{-1} \int_{-\infty}^{+\infty} I(\omega)\, e^{i\omega(t_1 - t_2)}\, d\omega, \quad (10)$$

from which it follows that the correlation function differs from zero only if $t_1 - t_2 \lesssim (\Delta\omega)^{-1}$. During this time the field can be regarded as differing little from coherent. The quantity $\Delta t = (\Delta\omega)^{-1}$ determines essentially the effective time of the elementary act of transition and the time of establishment of the stationary state of interaction between the radiation field and the quantum system.

Indeed, it follows from (5), (6), and (9) that the probability P_{mn} of the transition $m \to n$ per unit time (that is, the absorption intensity) can be written in the form

$$P_{mn}(t) = \frac{dW_{mn}(t)}{dt} = \hbar^{-2} |d_{mn}|^2 \int_0^t dt' \Phi(t, t') \times \{\exp[i\omega_{nm}(t - t')] + \exp[-i\omega_{nm}(t - t')]\}. \quad (11)$$

The values of $\Phi(t, t') = \Phi(t - t')$ decrease rapidly if t' differs from t by an amount larger than $(\Delta\omega)^{-1}$. Therefore, the intensity of absorption at a given instant t is determined not by the total time of action of the exciting radiation, from 0 to t, but only by the action during a certain interval $\sim(\Delta\omega)^{-1}$ preceding the instant t. Further, the sharpness of the function $\Phi(t, t')$ enables us to replace the lower limit in the integral (11) by ∞ when $t \gg (\Delta\omega)^{-1}$. Then, taking (10) into account, we get

$$P_{mn} = \hbar^{-2} \cdot 8\pi |d_{mn}|^2 c^{-1} I(\omega_{nm}), \quad (12)$$

$$\overline{W}_{mn}(t) = P_{mn}\, t. \quad (13)$$

This means that a stationary interaction mode is established between the radiation and the quantum system after a time interval t of the order of $(\Delta\omega)^{-1}$ following the start of the action of the radiation. This mode is characterized by the fact that the transition probability per unit time is constant, and the total probability of the $m \to n$ transition is proportional to t at the instant of time t.

On the basis of the foregoing, the time $\Delta t = (\Delta\omega)^{-1}$ can be interpreted as the effective duration of the elementary absorption act.[12] This interpretation agrees with the classical notion that the field is an aggregate of individual wave packets interacting with the atom during a time equal to the reciprocal of their spectral width[8].

The case of interaction between the system and a monochromatic field can be obtained by going to the limit as $\Delta\omega \to 0$ in the expressions written out above. Then (8) and (10) yield

$$\overline{W}_{mn}(t) = 8\pi |d_{mn}|^2 \cdot 4I(\omega) \hbar^{-2} c^{-1} \times (\omega - \omega_{nm})^{-2} \sin^2(\omega - \omega_{nm}) \frac{t}{2}. \quad (14)$$

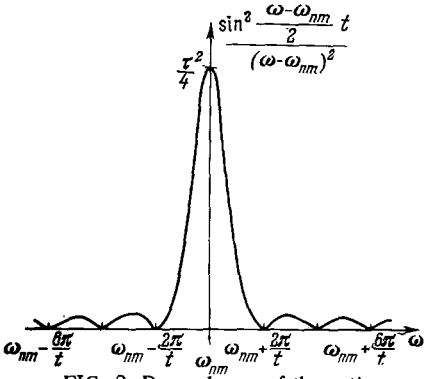

FIG. 2. Dependence of the ratio $\sin^2 \frac{\omega - \omega_{nm}}{2} t \Big/ (\omega - \omega_{nm})^2$ on the frequency ω.

Figure 2 shows a plot of $\sin^2[(\omega - \omega_{nm})t/2]/(\omega - \omega_{nm})^2$ against the frequency ω of the exciting radiation. The height of the principal maximum, which determines the probability of finding the system in the state n by the instant t under the action of the resonant field ($\omega = \omega_{nm}$), increases in proportion to t^2. The appreciable probability of the system transition $m \to n$ is retained in the interval $\omega = \omega_{nm} \pm 2\pi/t$. In other words, for each frequency ω there exists a time range $t \approx 2\pi/|\omega_{nm} - \omega|$, within which the probability of the transition $m \to n$ is of the same order as in resonant excitation. Such a frequency dependence of $\overline{W}_{mn}(t)$ on ω can be regarded also as a manifestation of the complex spectrum of a harmonic oscillation restricted to a time t, and as a reflection of the fact that the law of conservation of energy is satisfied within the time interval t of the interaction between the quantum system and the radiation field only accurate to within the energy uncertainty relation $\Delta E t \gtrsim \hbar$. Only in the limiting case as $t \to \infty$ does the requirement of the energy conservation law lead to the possibility of excitation of the transition $m \to n$ of only one resonant harmonic $\omega = \omega_{nm}$.

In the foregoing analysis we disregarded the finite width of the energy levels of the quantum system, that is, the finite lifetime at the levels m and n. In the simplest case such an account can be carried out under the assumption that the k-th state decays like $\exp(-\Gamma_k t)$, where Γ_k^{-1}—lifetime of this state. Then the distribution of the energy of the system in the k-th state is described by a Lorentz function

$$W_k(E) = \frac{\hbar\Gamma_k}{2\pi} \left[(E - E_k)^2 + \frac{\hbar^2 \Gamma_k^2}{4} \right]^{-1}, \quad (15)$$

and the expression for the amplitudes of the states (6) remains valid when E_k is replaced by $E_k - (i\hbar\Gamma_k/2)$[4]. It can be shown that in this case, for sufficiently long times t ($t \gg \Gamma_{nm}^{-1}$), after the nonstationary processes have terminated, the transition probability $W_{mn}(\infty)$ is equal to*

*The quantity $W_{mn}(\infty)$ is defined here as the ratio of the total absorbed energy to the transition energy $\hbar\omega_{nm}$.

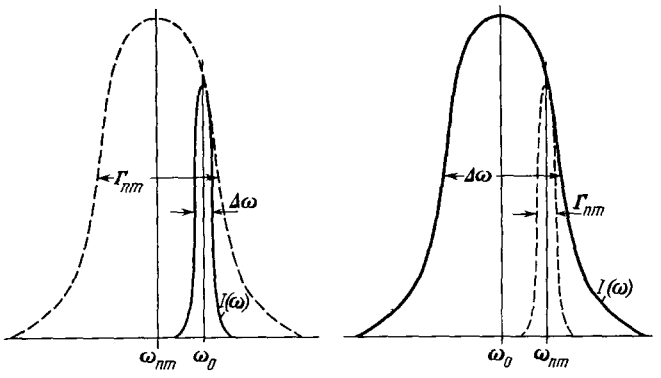

FIG. 3. Resonant excitation by radiation with "narrow" (a) and "broad" (b) spectrum.

$$W_{mn}(\infty) = 8\pi |d_{mn}|^2 c^{-1}\hbar^{-2}\Gamma_m^{-1} \times \int_{-\infty}^{+\infty} 2\Gamma_{nm} \left\{ \frac{I(\omega)}{[(\omega-\omega_{nm})^2 + \Gamma_{nm}^2]} \right\} d\omega, \quad (16)$$

where $\Gamma_{nm} = (\Gamma_n + \Gamma_m)/2$. The result of integration depends essentially on the ratio of the width of the spectral distribution $\Delta\omega$ of the function $I(\omega)$ to the sum of the natural half-widths of the levels m and n (Γ_{nm}). Let us consider two limiting cases of excitation of a system by radiation with a "narrow" and "wide" spectrum. In the former case $\Delta\omega \ll \Gamma_{nm}$, that is, the spectrum of the exciting radiation is situated in a region which is narrow compared with Γ_{nm} near the frequency ω_0 (which generally speaking is not equal to ω_{nm}, see Fig. 3a). Then

$$W_{mn}(\infty) = 16\pi |d_{mn}|^2 I_0 \Gamma_{nm} c^{-1}\hbar^{-2}\Gamma_m^{-1} \times [\Gamma_{nm}^2 + (\omega_0 - \omega_{nm})^2]^{-1}, \quad (17)$$

where

$$I_0 = \int_{-\infty}^{+\infty} I(\omega)\, d\omega$$

is the total excitation intensity. The contour of the absorption line is Lorentzian with half-width Γ_{nm} [cf. (15)]. In the case $\Gamma_m \gg \Gamma_n$ and $|\omega_0 - \omega_{nm}|^2 \ll \Gamma_m^2/4$, the quantity $W_{nm}(\infty)$ is proportional to Γ_m^{-2}, that is, the square of the lifetime of the initial state m. This corresponds to the fact that when $\Delta\omega \ll \Gamma_m$ the effective duration of the process of absorption by a single quantum system $\Delta t = (\Delta\omega)^{-1}$ is much longer than the lifetime of the initial state Γ_m^{-1} and that the probability of absorption of a photon with frequency $\omega_0 \approx \omega_{nm}$ is proportional to the square of the time [see formula (14) and Fig. 2].

In the second case of excitation with radiation with a "broad" spectrum $\Delta\omega \gg \Gamma_{nm}$ (Fig. 3b), the quantity $I(\omega)$ can be regarded as constant in the frequency region near ω_{nm} ($I(\omega_{nm})$), where the integral in (16) differs from zero. Then

$$W_{mn}(\infty) = 16\pi^2 |d_{mn}|^2 I(\omega_{nm})\, c^{-1}\hbar^{-2}\Gamma_m^{-1}. \quad (18)$$

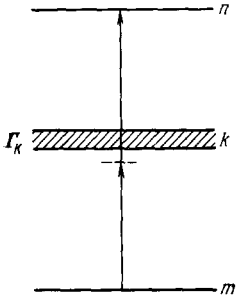

FIG. 4. Three-level scheme of two-photon transition.

It follows from this expression that if the effective time of absorption $\Delta t = (\Delta\omega)^{-1}$ is much shorter than the lifetime of the initial state Γ_m^{-1}, then, accurate to a factor 2π, the transition probability $W_{mn}(\infty)$ is equal to the product of the probability of the transition $m \to n$ per unit time [see (12)] by the average lifetime of the system in the initial state Γ_m^{-1}. This corresponds to the fact that the main contribution to the transition probability is made by the time region $t \gg (\Delta\omega)^{-1}$ (but still $t \ll \Gamma_m^{-1}$), where the transition probability $\overline{W}_{mn}(t)$ is proportional to the time t, and the total absorption time is limited to Γ_m^{-1}.

3. Two-photon transitions (second-order processes). Before we proceed to consider the general laws of multiphoton processes, we emphasize some features of two-photon processes, using two examples. As a first example we consider in the dipole electrical approximation the transition of an atom from the lower state m into an upper state n with absorption of two photons from the radiation field E(t). For simplicity we assume that in addition to the initial and final levels there is only one additional level k with energy E_k and damping Γ_k (Fig. 4). Averaging the probability of the two-photon transition $\overline{W}_{mn}(t)$ over the time t, in accordance with (6), we get

$$\overline{W}_{mn}(t) = \overline{|a_{nm}^{(2)}(t)|^2} = \hbar^{-4} |d_{mk}|^2 |d_{kn}|^2 \times \int_0^t dt_1 \int_0^{t_1} dt_2 \int_0^t dt_3 \int_0^{t_3} dt_4 \langle E(t_1) E(t_2) E^*(t_3) E^*(t_4)\rangle \times \exp\{(i\omega_{nk} - \Gamma_k/2) t_1 + (i\omega_{km} + \Gamma_k/2) t_2 - (i\omega_{nk} + \Gamma_k/2) \times t_3 - (i\omega_{km} - \Gamma_k/2) t_4\}. \quad (19)$$

The only characteristic of the field which must be known for the calculation of $\overline{W}_{mn}(t)$ is the fourth-order moment $\mu_4 = \langle E(t_1)E(t_2)E^*(t_3)E^*(t_4)\rangle$. Under a normal (Gaussian) distribution of the field E(t), the fourth moment can be expressed completely in terms of the correlation functions. If the field intensity does not depend on the time, then[13]

$$\mu_4 = \Phi(t_1 - t_2)\Phi(t_3 - t_4) + \Phi(t_1 - t_3)\Phi(t_2 - t_4) + \Phi(t_1 - t_4)\Phi(t_2 - t_3), \quad (20)$$

where $\Phi(t_a - t_b)$ is given by (10).

In interpreting the terms of the series (6), which give the second approximation, we have already noted that the time intervals $t_1 - t_3$ and $t_2 - t_4$ (as well as $t_1 - t_4$ and $t_2 - t_3$, which correspond to replacing t_3 by t_4 in Fig. 1c), play the roles of the times of transition of the atom from the initial to the intermediate and from the intermediate to the final state, while the gap between these intervals is the time between the individual transitions in the two-photon process. Inasmuch as $\Phi(t_a - t_b)$ differs essentially from zero only in the time interval $\Delta t = (\Delta\omega)^{-1}$ when the radiation field is coherent, the durations of the individual transitions, as in the case of the single-photon processes, cannot be essentially larger than $(\Delta\omega)^{-1}$ (this statement can be proved more rigorously). As to the time interval between the individual transitions, it is determined by the requirement that the energy conservation law be satisfied for the system "atom + radiation field," and can be much shorter than $(\Delta\omega)^{-1}$.

We assume first that the excitied field is monochromatic and has a frequency $\omega \approx \omega_{nm}/2$, and that $E_k \approx (E_n - E_m)/2$. It then follows from (10), (19), and (20) that

$$\overline{W}_{mn}(t) = 512\pi^2 I^2(\omega) |d_{mk}|^2 |d_{kn}|^2 c^{-2}\hbar^{-4} \times \frac{\sin^2(\omega_{nm} - 2\omega)t/2}{[(\omega_{km} - \omega)^2 + \Gamma_k^2/4](\omega_{nm} - 2\omega)^2}. \quad (21)$$

The quantity $\overline{W}_{mn}(t)$ differs markedly from zero only when $\omega_{nm} = 2\omega$, and is proportional to the square of the field intensity $I(\omega)$ and the product of the squares of the matrix elements $|d_{mk}|$ and $|d_{kn}|$. Such a transition $m \to n$ can be regarded as a sequence of elementary transitions $m \to k$ and $k \to n$, in each of which one photon is absorbed. It is important, however, that the photon absorption acts cannot be regarded as independent. Indeed, were they to be independent, the probability $\overline{W}_{mn}(t)$ would coincide with the product of the probabilities of the individual transitions, and the second resonant factor in the denominator would be not $(\omega_{nm} - 2\omega)^2$, but $[(\omega_{nk} - \omega)^2 + \Gamma_k^2/4]$ [see (17)]. The presence of two factors of this type would signify that the energy conservation law is satisfied in each elementary absorption act and that the transition $m \to n$ can be caused with approximately equal probability by any two photons with frequency lying in an interval of width Γ_k near $\omega_{nm}/2$. On the other hand, the presence of the factor $(\omega_{nm} - 2\omega)^2$ reflects the requirement of obligatory conservation of energy (for $t \to \infty$) only for the entire two-photon process.

The two-photon process considered above calls for the existence of an intermediate state, which is connected with the initial and final states by nonzero matrix elements. Frequently the intermediate states of a quantum system are divided into real and virtual[14], the latter being distinguished for the fact that they do not satisfy (as is customarily assumed) the energy conservation law. (In our case the virtual state would be the state k, for which $|E_k - E_m - \hbar\omega| \gg \Gamma_k$.) From the classical point of view, foregoing the energy conservation law makes the virtual state physically meaningless. However, quantum representations make it possible to present a different treatment of the intermediate states, without separating them into real and virtual with respect to satisfying the energy conservation law[15,16]. Indeed, in our analysis of the single-photon processes we noted that, as a result of the energy uncertainty relation, the probability of finding an atom in the state k within a time interval $\Delta t_k \approx 2\pi/|\omega_{kn} - \omega|$ is approximately the same order as when $\omega = \omega_{km}$ for any arbitrarily large deviation of the frequency ω from the resonant frequency ω_{kn}. Therefore, when $|\omega - \omega_{km}| \gg \Gamma_k$ the interval Δt_k can be regarded as the lifetime of the atom in the intermediate state k; although $\omega \neq \omega_{km}$, the energy conservation law is not violated from the quantum point of view. At the same time, inasmuch as for the entire two-photon process the energy conservation law should be satisfied (as $t \to \infty$), the second photon should be absorbed within a time Δt_k.

Therefore, the shorter the time that the atom is in the intermediate state, the smaller should be the probability of the two-photon transition. This follows indeed from (21), which shows that when $|\omega_{km} - \omega| \gg \Gamma_k$ the quantity $\overline{W}_{mn}(t) \sim \Delta t_k^2$. The quadratic character of the dependence can be readily understood by recognizing that in our case $\Delta t_k \ll (\Delta\omega)^{-1}$ [see formula (14) and Fig. 2].

We note that the inequality $|\omega_{km} - \omega| \gg \Gamma_k$ or $\Delta t_k \ll \Gamma_k^{-1}$ corresponds to the fact that the lifetime in the k-th level is determined not by relaxation processes, but by the requirement of energy conservation within the limits of the uncertainty relation. It is natural here that the quantity $\overline{W}_{mn}(t)$ does not depend on Γ_k^{-1}. To the contrary, if $|\omega_{km} - \omega| \ll \Gamma_k$, then $\Delta t_k \gg \Gamma_k^{-1}$ and the lifetime at the k-th level (and consequently also $\overline{W}_{mn}(t)$) is determined by relaxation processes. Thus, depending on the sign of the inequality written out above, the levels can be separated, if necessary, into real and virtual; the energy conservation law, however, is satisfied for both.

We assume now that the transition $m \to n$ is excited by two harmonics with frequencies ω_1 and ω_2, such that $\omega_1 + \omega_2 \approx \omega_{nm}$ and $\omega_{km} - \omega_{1,2} \gg \Gamma_k$. In this case, (19) yields

$$\overline{W}_{mn}(t) = \left(\frac{8\pi}{c}\right)^2 \frac{|d_{mk}|^2 |d_{kn}|^2}{\hbar^4} I(\omega_1) I(\omega_2) \times \left|\frac{1}{\omega_{km} - \omega_1} + \frac{1}{\omega_{km} - \omega_2}\right|^2 \frac{4\sin^2 \frac{\omega_{nm} - \omega_1 - \omega_2}{2} t}{(\omega_{nm} - \omega_1 - \omega_2)^2}. \quad (22)$$

This expression is similar to the relation for the probability of a two-photon transition via two intermediate states, differing in the fact that a photon ω_1 is absorbed in one of them and a photon ω_2 is absorbed in the other, i.e., a two-photon transition with a different photon absorption sequence. It is important that

the probability of such a transition is not equal to the sum of the probabilities of the transitions via the two possible intermediate states. Formula (23) shows that to determine $W_{mn}(t)$ it is first necessary to add the amplitudes of the probabilities of the possible transition paths, and then form the square of the modulus of the sum of these amplitudes. We get an "interference of probabilities," as a result of which the probability of the two-photon process can vary from zero to the square of the sum of the amplitudes of the probabilities of the transitions along the different paths. Thus, the total probability $\overline{W}_{mn}(t) = 0$ when the levels are strictly equidistant, $\omega_{km} - \omega_1 = \omega_2 - \omega_{km}$, that is, two-photon transitions $m \rightarrow n$ are impossible (this result is valid only when $\Gamma_k = 0$).

The "interference of probabilities" is a manifestation of the ambiguity of the transition path between two states in the two-photon transition. In this case this ambiguity is connected with the fact that in principle we cannot tell which of the photons (ω_1 or ω_2) is the first to be absorbed, if all we know is that the system has gone over from the state m into n. Such an ambiguity (and consequently, the "interference of probabilities") disappears if the intermediate level is resonant for one of the photons. Indeed, if $|\omega_{km} - \omega_1| \rightarrow 0$, then the second term in (22) with the nonresonant denominator $\omega_{km} - \omega_2$ can be neglected.

Let us examine, finally, the excitation of an atom with intermediate level $E_k = (E_n - E_m)/2$ by radiation having a spectral width $\Delta\omega \gg \Gamma_k$ near the frequency $\omega = \omega_{nm}/2$. Then (19) yields

$$\overline{W}_{mn}(t) = (16\pi)^2 |d_{mk}|^2 |d_{kn}|^2 I^2(\omega_{km})\, c^{-2}\hbar^{-4}\Gamma_k^{-1} t. \qquad (23)$$

As in the case of the single-photon transition, the two-photon transition probability is proportional to the time t, and we can therefore introduce the concept of transition probability per unit time, independent of the time. Formally expression (23) can be represented, accurate to a factor 2π, as a product of the probabilities of the transitions $m \rightarrow k$ and $k \rightarrow n$ [see (12) and (18)]. This result is a consequence of the fact that when $\Delta\omega \gg \Gamma_k$ the stationary mode of excitation is established within a time $(\Delta\omega)^{-1} \ll \Gamma_k^{-1}$. In this mode, the probability of the transition $k \rightarrow n$ per unit time is proportional to the population of the level k, and the latter is proportional to Γ_k^{-1}. We note, however, that in the individual two-photon transition act the absorption of the individual photons cannot be regarded as independent. This corresponds mathematically to the fact that (22) cannot be represented in the form of a product of probabilities of absorption of individual photons.

By way of a second example of a two-photon process, let us consider resonant scattering of light by an atom having two nondegenerate levels m and n. For this process there is a complete theory, which makes use of the quantization of the radiation field. For sufficiently large times t, when all the transient processes have terminated, the probability that a photon ω_ρ of incident radiation will be absorbed and a photon ω_σ will be emitted, while the atom will again assume the initial state (m) [see[17], formula (37a)], is equal to

$$W_{\rho\sigma} = |V_{mn}^{(\rho)}|^2 |V_{nm}^{(\sigma)}|^2 \hbar^{-4} [\gamma_m^2 + (\omega_\rho - \omega_\sigma)^2]^{-1} [\gamma_n^2 + (\omega_{nm} - \omega_\sigma)^2]^{-1}, \qquad (24)$$

where $V_{mn}^{(\rho)}$ and $V_{nm}^{(\sigma)}$—matrix elements for the absorption of the photon ω_ρ and emission of the photon ω_σ, while γ_m and γ_n are the half-widths of the levels m and n. This formula was obtained for nondegenerate radiation, when the induced transitions from the upper to the lower levels can be neglected. In this case $2\gamma_n$ is the natural width of the level n, defined by the spontaneous transitions, and the width of the initial level $2\gamma_m$ is determined by the finite time that the atom will stay in the initial state in the presence of the radiation field ($\gamma_n \gg \gamma_m$).

Let us consider the shape of the absorption and emission lines in the two limiting cases of "narrow" ($\Delta\omega \ll \gamma_n$) and "broad" ($\Delta\omega \gg \gamma_n$) excitation spectra. In the former case the spectral density $I(\omega)$ differs from zero in a narrow spectral interval near the frequency ω_0 (see Fig. 3a). We obtain the total absorption probability by integrating (24) over all values of the frequency ω_σ, which yields

$$W_\rho = \text{const} \cdot I(\omega_0)\gamma_n [\gamma_n^2 + (\omega_{nm} - \omega_0)^2]^{-1}. \qquad (25)$$

It follows therefore that the shape of the absorption line contour is Lorentzian with half width γ_n.

We obtain the emission line shape by integrating (24) over all values of ω_ρ. Since $\gamma_m \ll \gamma_n$ for all ω_σ differing from ω_ρ by an amount larger than γ_m, the value of $W_{\rho\sigma}$ is likewise practically zero if $\Delta\omega \gg \gamma_m$

$$W_\sigma = \text{const} \cdot I(\omega_\sigma) [\gamma_n^2 + (\omega_{nm} - \omega_\sigma)^2]. \qquad (26)$$

It follows therefore that the emission line width coincides with the line width of the exciting light and is much narrower than the natural linewidth $2\gamma_n$ of the spontaneous emission. Inasmuch, furthermore, as the denominator in (26) remains practically constant within the confines of the line $I(\omega_\sigma)$, the integral intensity of the scattered light decreases with increasing $|\omega_{nm} - \omega_0|$ in the same way as the intensity of the spontaneous emission. This means that the resonant scattering of radiation with a "narrow" spectrum cannot be regarded as two successive independent processes, for otherwise the atom would not "remember" which of the photons was absorbed, and the spectrum of the scattered light would coincide with the spectrum of spontaneous emission. This result can be easily understood by using the classical representation of the atom as a harmonic oscillator with damping γ_n. Such an oscillator is excited by harmonics with frequencies lying in the interval $2\gamma_n$, and its stationary oscillations correspond only to the frequency of the driving force.

In the case of the scattering of light with a "broad" spectrum, the shape of the absorption line is given by the expression

$$W_\rho = \text{const} \cdot I(\omega_\rho)\, \gamma_n \gamma_m^{-1} [(\omega_{nm} - \omega_\rho)^2 + \gamma_n^2]^{-1}, \quad (27)$$

and the shape of the emission line

$$W_\sigma = \text{const} \cdot \gamma_n [(\omega_{nm} - \omega_\sigma)^2 + \gamma_n^2]^{-1}, \quad (28)$$

and both coincide with the shape of the spontaneous emission line. Consequently, in this case the resonance scattering as a whole can be regarded as consisting of two independent processes—absorption of the photon ω_ρ and succeeding emission of the photon ω_σ.*

As in the case of resonant scattering of radiation with a "narrow" spectrum, the result obtained can be understood by using the classical ideas. Indeed, as shown above, the time $\Delta t = (\Delta\omega)^{-1}$ is the effective absorption time. When $\Delta\omega \gg \gamma_n$, this time is much shorter than the lifetime of the atom in the excited state n. Therefore the atom is excited practically instantaneously, and then radiates like a freely vibrating oscillator with a de-excitation time constant γ_n^{-1}.

4. General characteristics of multiphoton processes. Having examined by means of the two examples the features of two-photon processes, we present without proof a formula for the transition probability per unit time—in which p-photons participate simultaneously. It is the result of solving equations of the type (6) for the probability amplitudes $a_n(t)$ under the assumption that when $t = 0$ the system is in one of unperturbed stationary states m.[14] By system we mean here the aggregate "atom + radiation field," and the energy of the system is made up of the energy of the radiation field, the energy of the atom, and the energy V of their interaction, the latter being regarded as a small perturbation. To calculate the probability of the p-photon transition, we first obtain, by perturbation theory, the amplitude of the final discrete state $a_n(t)$ in the p-th order. This expression, when written out in general form, is complicated and difficult to interpret. It can be simplified if we bear in mind that in most cases of practical interest of multiple-photon transitions, the final state is not one discrete state, but a group of closely-lying states. Then physical interest attaches to the probability of observing the system in any of the states of this group. In the p-photon transition this probability increases linearly with time, so that we can speak of the transition probability per unit time, which turns out to be[14]

$$W_{mn}^{(p)} = 2\pi\hbar^{-1} |K_{mn}^{(p)}|^2 \varrho_n, \quad (29)$$

where ρ_n—density of the final states near the energy $W_n \approx W_m$ of the unperturbed system, and $K_{mn}^{(p)}$—compound matrix element of order p:

$$K_{mn}^{(p)} = \sum_{k', k'', \ldots, k^{(p-1)}} \frac{V_{mk'} V_{k'k''} \ldots V_{k^{(p-1)}n}}{(W_m - W_{k'})(W_m - W_{k''}) \ldots (W_m - W_{k^{(p-1)}})} \cdot \quad (30)$$

*On the other hand, the elementary acts of absorption and emission of individual photons are interdependent [see (24)].

Here W_n—energy of the unperturbed system in the state n, and V_{ab}—matrix element between the states a and b of the interaction operator V. Formula (29) differs from the corresponding formula for the single-photon transition probability only in that the matrix element of V_{mn} of the direct transition is replaced by the compound matrix element $K_{mn}^{(p)}$ of order p. Its numerator contains the product of p matrix elements of the form V_{ab}: the first matrix element starts with the initial state m, and the latter arrives at the final state n. The denominator $K_{mn}^{(p)}$ contains the product of $(p - 1)$ energy differences between the initial and the intermediate states. The structure of relations (29) and (30) gives grounds for regarding the p-photon transition as occurring in p stages via $(p - 1)$ real intermediate states of the unperturbed system: one photon is first absorbed (or emitted), leaving the system in a state k′, followed by absorption (or emission) of a second photon, bringing the system to the state k″, etc. Finally, as a result of elementary single-photon acts, the system is in the final state n. The quantity $[(W_m - W_{k'})(W_m - W_{k''}) \ldots (W_m - W_{k(p-1)})]^{-1}$ (in analogy with the particular example considered above) is proportional to the product of $(p - 1)$ effective times during which the system is in the $(p - 1)$ intermediate states. The cases when the energy differences vanish call for an evaluation of the finite lifetimes of the intermediate states (two such cases—a stepwise two-photon transition and resonance fluorescence—were considered earlier). Thus, the calculation of the probability of the multiphoton transition reduces to the calculation of the matrix elements of single-photon transitions via the intermediate states. Generally speaking, it is necessary to know the matrix elements of the transitions via all the intermediate states, something greatly complicating the problem compared with the calculation of the probability of the single-photon transition. However, it is frequently sufficient to take into account only the intermediate states that make the maximum contribution to the multi-photon process.

Relation (29) allows us to draw several important conclusions concerning the characteristic features of the multiphoton transitions, without determination of the exact values of the matrix elements. These include the following:

1) The probability of the p-photon transition differs essentially from zero only if the energy conservation law is satisfied for the entire process as a whole, but, unlike in the single-photon transition, photons can be emitted in a multiphoton process also if the resultant transition of the atom is to either a lower or a higher energy state.

2) In the case of a transition with absorption of p-photons of equal frequency, the quantity $W_{mn}^{(p)}$ is proportional to the number of photons of this frequency, raised to the degree p, that is, to the emission intensity raised to the degree p.

3) The maximum contribution to the probability of the multiple-photon transition is made by the resonant

intermediate states, for which $W_m \to W_{k(k)} \to 0$. Thus, in the case of a two-photon transition, it is sufficient to leave in (30) only one resonant term.

4) The selection rules for multiphoton transitions differ from the selection rules for single-photon transitions. In systems with a symmetry center, dipole electric transitions in which an even number of photons participate are allowed only between states having equal parity, and those with participation of an odd number of photons are allowed between states of opposite parity.

5) If there are not one but several intermediate states of the type k', k'', ..., $k^{(p-1)}$, then the additive quantities are not the probabilities but the amplitudes of the probabilities of the different possible paths of the p-photon transition. This peculiarity of multiphoton transitions is connected both with the fact that in principle it is impossible to distinguish between the photon absorption and emission sequences and with the fact that, in principle, for a given photon absorption and emission sequence, transitions via different intermediate states of the system are possible.

3. General Review of Experiments on Multiphoton Processes

The volume of experimental material on single-photon processes accumulated by now is so large, that it is advantageous to present only a brief general review, and consider in more detail problems of greatest interest from the theoretical and experimental points of view. Although such multiphoton phenomena as resonance fluorescence or Rayleigh and Raman scattering were known long ago and were analyzed theoretically in detail, the special interest in multiphoton processes as a whole arose and developed during the last decade in connection with the observation of phenomena connected with the absorption of several photons of the exciting radiation in a single elementary act, first in the radio band and then in the optical band.

In most of the earlier papers devoted to such induced multiphoton transitions, principal attention was paid to the extent to which the experimental results correspond to the theoretical predictions. Rarefied systems with discrete energy spectra are in this sense the most interesting. The possibility of investigating multiphoton phenomena in discrete atomic systems in the optical band, are at present essentially limited by the lack of generators of stimulated emission in the optical band with adjustable frequency. Because of the relative simplicity of producing sufficiently intense radiation sources in the radio band, the relatively large number of systems that are convenient for the observation of multiphoton transitions, and the possibility of varying the positions of the most energetic levels over a sufficiently wide range (the Zeeman and Stark effects), the main results on quantitative experimental and theoretical investigations of multiphoton phenomena were obtained at radio frequencies (see, for example,[18-29]). A systematic study of multiphoton transitions, aimed at checking the correspondence between the theoretical and experimental results, is the subject of[21,26]. A distinguishing feature of the experimental study of multiphoton transitions in the radio band, using rarefied systems, is the need for creating a non-equilibrium distribution of the populations of the sublevels of the investigated transition, inasmuch as in the radio band we have $|E_n - E_m| \ll kT$, so that in the state of thermodynamic equilibrium the populations of the initial and final levels are practically identical. In[21] there were investigated multiphoton transitions between the sublevels of the ground state of potassium vapor, and the necessary population difference was attained by the molecular beam method. In[26], in an investigation of multiphoton transitions between sublevels of the ground state of sodium vapor, the necessary population difference was produced by the optical-orientation method[29]. The main results of the investigation can be briefly formulated in the following fashion: in all cases when it is possible to make a sufficiently accurate comparison of the experimental results with the theoretical ones, the theoretical predictions were fully confirmed by experiment (see Chapter II, Sec. 1).

An investigation of multiphoton transitions in the optical band, using laser emission, is of great interest from two points of view. It is possible to use this method, first, to investigate transitions between states having identical parity, that is, transitions which are forbidden in single-photon processes (see[30-42], Chapter I). Second, if the structure of the levels and the matrix elements of the transitions in the investigated system are sufficiently well known, then the investigation of multiphoton processes can yield additional information on the statistical properties of the laser emission[43], inasmuch as processes of second and higher orders are determined by moments of fourth and higher orders of the radiation field, respectively. Unlike the usual radiation of incoherent sources, there are no theoretical grounds whatever for assuming that the radiation of the laser obeys a Gaussian (normal) distribution law.[44]

In systems with a continuous spectrum, such as metals and semiconductors, where a theoretical analysis of multiphoton transitions is very complicated even now, and apparently cannot be carried out with the accuracy required for comparison with the experimental results[45,46], it is of interest to observe such phenomena as two-photon internal and external photoeffects. The internal two-photon photoeffect in a semiconductor, which consists in exciting electrons from the valence band to the conduction band, was observed in[47] in CdS using a ruby laser. The energy of the photons of the ruby laser (1.8 eV) is insufficient to excite the electrons in the conduction band (the energy gap between bands is 2.4 eV), so that for ordinary

radiation sources with the wavelength of the ruby laser this semiconductor is transparent. Two-photon excitation of electrons in the conduction band was detected by observing recombination emission from the exciton and impurity levels, arising as a result of two-photon excitation. The intensity of the recombination emission has exhibited a quadratic dependence on the excitation intensity, and has coincided in order of magnitude with the theoretically predicted value. In[45,48] are discussed the possibilities of using two-photon processes in semiconductors for the detection of weak infrared radiation.

Theoretical estimates of the external surface and volume two-photon photoeffects in metals and semiconductors[49-52] show that in principle it is possible to observe such an effect at intensities afforded by pulsed solid-state lasers. A study of these phenomena is essential for the investigation of the red shift of the photoeffect at large radiation densities, but its observation is made exceedingly difficult by thermionic emission[53] and, as far as we know, has not yet been made.

Of interest from both the theoretical and experimental aspects is the possibility of two-photon ionization of atoms by laser radiation; it is complicated, however, by the fact that the minimum energy of ionization from the ground state, 3.89 eV for cesium, exceeds the two-photon energy of the available high-power lasers. Such an effect can be observed in the negative ions I^-, Br^-, and F^-, which have an ionization potential that is sufficiently low for two-photon excitation with the aid of a ruby laser[54]. The development of techniques of nonlinear effective frequency conversion in lasers (generation of a second harmonic, stimulated Raman scattering, see Chapter III, Sec. 3) uncovers new and broad possibilities for the investigation of two-photon photoionization of atoms. An investigation of multiphoton absorption processes in both the radio and the optical bands has shown (see Chapter II) that these processes can be described quite adequately in terms of the number of photons and populations of the states of the quantum system. The physical simplicity and clarity of the model of multiphoton interaction are very convenient for the description of the nonlinear character of the interaction between radiation and matter. However, an investigation of multiphoton processes connected with the scattering of radiation by quantum systems (such as the generation of harmonics, parametric amplification, parametric generation, and Raman scattering) has shown that these processes are strongly influenced by the phase relations between the harmonics of the exciting and scattered radiation. The phenomena observed in this case cannot be described in terms of the number of photons and state populations only (see Chapter III, Section 1). These phenomena can be divided into two principal types: interference phenomena, which take place in the elementary multiphoton act of scattering by each isolated center of the scattering system, and interference phenomena, connected with the specific nature of scattering by the entire ensemble of scattering centers. Phenomena of the first type were observed in investigations of resonance fluorescence[55-62] and were manifest in a sharp change of the intensity of the scattered light in the so-called "level crossing" effect and modulation of the fluorescence light intensity (see Chapter III, Sec. 2). Phenomena of the second type were observed both in the radio band and in the optical band (Chapter III, Sec. 3).

In the radio band these effects were observed in three-level gas masers of the microwave band[63-66] and have led to distortion of the spectral-line shape of the generated radiation; they were also observed in generation of harmonics[67-76]. The efficiency with which harmonics were generated under certain conditions turned out to be proportional to the square of the number of molecules of the active medium, and this was manifest in a sharp increase in the efficiency of generation over that obtained from the elementary acts of generation on each molecule of the medium. The most important application of multiple-photon processes in the radio band lies in obtaining harmonics in a band for which there are no other sources of coherent signals (frequency multiplication). It is probable that in the near future these effects will be the basis of new types of tunable amplifiers, mixers, limiters, and modulators for the millimeter and submillimeter bands.

In the optical band, interference phenomena of the second type were observed in second harmonic generation (SHG) with a ruby laser. SHG was first realized successfully in quartz[77]; with the ruby laser having an average power of 10 kW, the second harmonic power was 1 mW. Further intense development of research on the mechanism of generation of optical harmonics in crystals and media in which such generation is effectively realizable[78-79] (see Chapter III, Sec. 3) has pointed out the importance of the phase relations between the fundamental and generated harmonics as they propagate in a crystal having optical dispersion. It was observed that the efficiency of generation of the harmonics depends not only on the intensity of the exciting radiation, but also on its direction of propagation in the crystal. It turned out that in some crystals there exist such directions, for which the SHG efficiency increases in proportion to the square of the crystal length, whereas for other directions it has an oscillating character. In these crystals it was possible to increase the SHG efficiency of a ruby laser to 20%[99], which makes it possible to attain in the nearest future megawatts of second harmonic in ruby and neodymium lasers. At the present time nonlinear processes in crystals are among the principal methods of effective conversion of the energy of laser emission in the short-wave part of the optical spectrum[100-103]. The development of Q-switched lasers has made it possible to generate *in crystals*

not only the second but also the third harmonic[104-105]. The maximum energy conversion efficiency in the third harmonic in calcite is 0.01%.

The mixing of optical frequencies in crystals uncover additional possibilities for optical frequency conversion in lasers. Optical mixing of the emission of two ruby lasers with somewhat different frequencies was first observed in[77]. Generation of the summary frequency of ruby and neodymium lasers was observed in[106]. In[107-109] there were proposed different schemes for the use of multiphoton processes in crystals for the construction of variable-frequency generators of coherent radiation in the optical band. Although theoretical estimates show that it is possible in principle to realize such systems at the contemporary laser intensities, such systems have not yet been realized at present.

Generation of difference optical frequency was first observed by mixing a beam from a ruby laser with an incoherent beam of a mercury lamp ($\lambda \approx 3115$ Å). The efficiency with which the difference frequency was generated, as expected, was negligible; with the power in the 3115 Å mercury line amounting to about 2×10^{-4} W, the power radiated at the difference frequency was 10^{-10} W. The possible use of multiphoton phenomena in crystals for the creation of sources of coherent radiation in the far infrared and in the microwave bands is discussed in[110-113].

A study of the nonlinear processes of frequency conversion in crystals is of considerable interest for the investigation of the properties of the crystals themselves: dispersion, symmetry properties, quantitative determination of the coefficients of nonlinear optical polarizability, of the position and intensities of the absorption bands. An original effect of inducing a dc voltage by laser light, corresponding to the limiting case of generation of a zero difference frequency, was observed in[114]. This effect is of interest because its magnitude can be quantitatively predicted from known optical properties of the crystal; its observation makes it possible to increase the accuracy of measurement of the coefficients of nonlinear polarizability of the crystals.

The high radiation densities attainable through the use of lasers have made it possible to check experimentally the laws of nonlinear reflection of light on a boundary of a dielectric[115-117]. Investigation of the laws of nonlinear reflection and refraction is important for the understanding of the operation of optical systems at very high radiation densities.

Successful realization of second-harmonic generation using gas[96,118,119] and semiconductor[120,121] lasers of continuous action uncovers new possibilities for a quantitative investigation of multiphoton phenomena in crystals. When pulsed solid-state lasers are used, such investigations are made difficult by the presence of a random multiple-mode structure in their radiation. The possibilities of investigating the statistics of laser radiation by observing multiphoton phenomena in crystals are discussed in[43].

Considerable success in the investigation of the two-photon process of Raman scattering (RS) was attained by using a ruby laser as a source of light for the excitation of Raman scattering. The high intensity, the narrow width of the spectral line and the directivity of the laser radiation make lasers, along with the mercury lamp, one of the principal sources of radiation for the excitation of Raman spectra. The results obtained to date show that lasers have certain advantages over mercury lamps as sources for the excitation of Raman spectra when used to excite the spectra of small crystalline samples or gases, and also in some other special applications[122-125]. An important result of the use of a ruby laser for the investigation of Raman spectra is the determination of the absolute values of the cross section for Raman scattering of some lines of liquid benzene, nitrobenzene, and toluene[126].

Investigations of Raman scattering with the aid of lasers have led to a discovery of the effect of stimulated Raman scattering[127-135] (see Chapter IV, Sec. 3). The high intensity of scattering radiation in stimulated Raman scattering uncovers new possibilities for the investigation of Raman spectra (for example, the investigation of spectra of long-wave crystal oscillations[138]). The efficiencies for the conversion of power in stimulated Raman scattering already attained are of the order of 10—30% and bring this phenomenon to the forefront as one of the basic methods for the conversion of the laser-emission spectrum. The investigations of stimulated Raman scattering have shown that under thermodynamic equilibrium it is possible to convert efficiently the radiation power from a laser not only in the long-wave region of the spectrum (Stokes Raman scattering) but also in the short-wave region (anti-Stokes Raman scattering). The latter possibility is essentially connected with the presence of interference phenomena in Raman scattering (see Chapter III, Sec. 3), when Raman scattering can no longer be regarded as an incoherent two-photon process in which the phases of the excited molecular oscillations have a random distribution[136-145].

II. MULTIPHOTON PROCESSES REQUIRING NO ACCOUNT OF INTERFERENCE PHENOMENA

1. Multiphoton Transitions Between Zeeman Sublevels of the Sodium Atom[26]

1. Method of observing multiphoton transitions. The total angular momentum of the sodium atom, F, in the ground state, which consists of the spin of the nucleus (I = 3/2) and the spin of the electron shell (J = 1/2), assumes two values, F = 1 and F = 2, forming a Zeeman level structure in a weak magnetic field (Fig. 5a). In very weak magnetic fields, the level splitting depends linearly on the field intensity and all

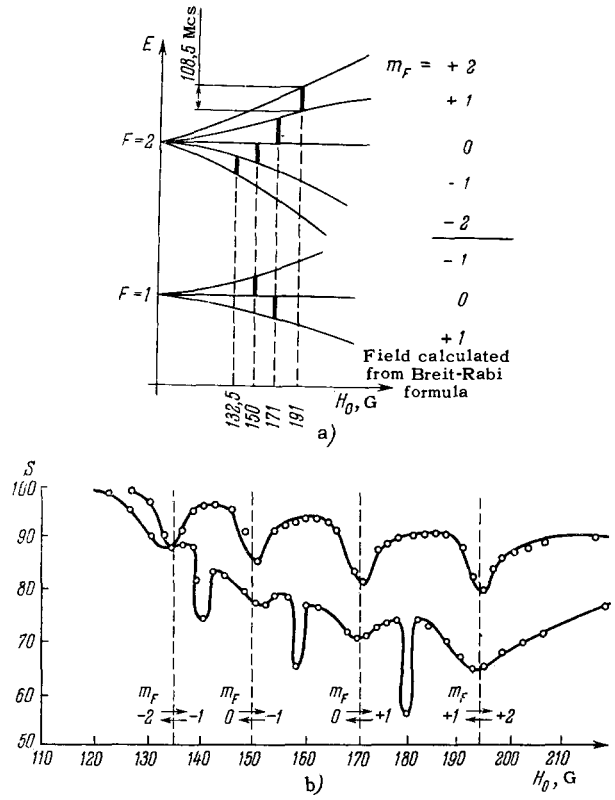

FIG. 5. a) Zeeman splitting of levels of the ground state of the sodium atom in a weak magnetic field. The resonant values of the magnetic field are those expected for the frequency 108.5 Mcs. b) Variation of the spectrum of the signal S with the intensity of the rf field. The lower curve corresponds to larger rf field amplitudes.

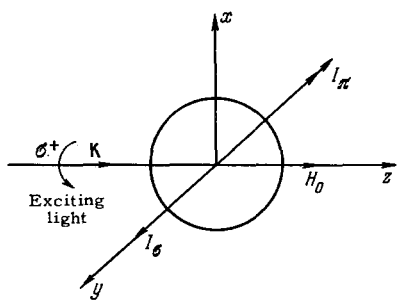

FIG. 6. Orientation of constant magnetic field H_0 relative to the direction K of the orienting light beam and the direction of detection of the scattered light, in experiments with optical pumping of sodium.

levels with F = 1 and F = 2 are equidistant. However, starting with fields on the order of 1 G, the deviation from equidistant spacing becomes larger than the relaxation width of the levels.

Multiple-photon transitions were observed only between sublevels with the same value of F. The reason for this is that, as follows from a theoretical analysis, the probability of transitions with $\Delta F \neq 0$ is very small compared with the probability of the transitions with $\Delta F = 0$. In fact, for the $\Delta F = 0$ transition, the composite matrix element $K_{mn}^{(p)}$ contains a term of the order of $(V_{ab})^p/\Delta\omega_1^{(p-1)}$, where $\Delta\omega_1$ is of the order of the deviation of the level spacing from equidistant. On the other hand, if $\Delta F \neq 0$, then $K_{mn}^{(p)}$ is of the order of $(V_{ab})^p/\Delta\omega_2^{(p-1)}$, where $\Delta\omega_2$ is of the order of magnitude of the hyperfine splitting. Inasmuch as $\Delta\omega_1 \ll \Delta\omega_2$, the value of $K_{mn}^{(p)}$ for transitions with $\Delta F \neq 0$ is negligibly small compared with $K_{mn}^{(p)}$ for transitions with $\Delta F = 0$. This corresponds to the fact that the times that the atom stays in the intermediate state of the p-photon transition $\Delta F = 0$ are much longer than the time for the transition $\Delta F \neq 0$. For this reason, multiphoton resonances $\Delta F \neq 0$ could never be observed. We note that this peculiarity of transitions with $\Delta F = 0$ and $\Delta F \neq 0$ is characteristic of multiphoton processes only; for a single-photon transition, the matrix elements $K_{mn}^{(1)}$ do not depend on the frequency and have an order of magnitude V_{ab} for both $\Delta F = 0$ and $\Delta F \neq 0$ transitions.

Under conditions of thermodynamic equilibrium, the relative difference in the populations of the sublevels having the same value of F is so small, that at the atomic concentrations employed (on the order of 10^{10}—10^{11} cm^{-3}), the absorption of photons of a radio-frequency (rf) field, connected with the transitions between sublevels, cannot be observed in practice. To produce an appreciable population difference, use was made of the known method of optical orientation, based on the difference in probabilities of excitation and de-excitation of atoms from different sublevels[29]. It was thus possible to produce a relative difference in populations of Zeeman sublevels, on the order of 10%. For direct observation of absorption of radio-frequency photons at the indicated atomic concentrations, this is still not enough, but their absorption can be observed indirectly, by determining the change in the optical properties of the medium for a radiation that orients the atoms. The point is that the absorption of photons from a radio-frequency field, which leads to a change in the sublevel populations, is accompanied by a change in the absorption and in the intensity of scattering of the orienting radiation. Owing to the large sensitivity of the optical-band receivers, this method makes it possible to observe exceedingly small changes in the absorption of the radio-frequency photons (in the limit, one transition in the radio-frequency band gives rise to a change in the light flux by one photon).

The orientation of the fields in the foregoing experiments with optical pumping is shown in Fig. 6. A spherical cell was filled with saturated sodium vapor (pressure 10^{-6} mm) and a buffer gas (argon) to reduce the effect of the disorientation of the Na atoms upon collision with the walls of the vessel (introduction of the buffer gas increased the time constant of the relaxation processes to 0.1 sec). The cell was exposed to resonant circularly-polarized light from a sodium lamp, propagating in the direction of the superimposed constant magnetic field H_0. The linearly polar-

ized (I_π) and the circularly polarized (I_σ) components of the resonance fluorescence were observed at a right angle to this direction. A measure of the number of transitions between the Zeeman sublevels was the quantity

$$S=\frac{I'_\pi}{I_\pi}-\frac{I'_\sigma}{I_\sigma}, \qquad (31)$$

where I_π and I_σ are the intensities of the π and σ components in the absence of an rf field, and I'_π and I'_σ were the corresponding intensities in the presence of the field; the latter was produced by special coils in which the cell was placed.

To observe the Zeeman transitions one could either fix the field intensity H_0 and vary the frequency ω of the rf fields, or else fix ω and vary H_0. In practice the latter method is more convenient, and was used to observe multiphoton transitions even in the early experiments, carried out at a constant frequency 108.5 Mcs.

According to the Breit-Rabi formula, four resonances corresponding to fields 132, 150, 171 and 192 Gauss were expected for the Zeeman splitting (two out of the six resonances that are possible within the limits of the sublevels F = 1 coincide with two resonances within the limits of F = 2, if we neglect the very small difference, due to the nuclear spin, between the Zeeman splittings of these sublevels). These resonances were actually observed in weak radio-frequency fields. With increasing amplitude of the radio-frequency field, narrow additional resonance lines appeared (see Fig. 5b). It turned out that the frequencies of these additional resonances are the arithmetic means of the frequencies of two neighboring resonances observed in weak rf fields. Inasmuch as each rf photon causes transitions with a change $\Delta m_F = \pm 1$ (the rf field in these experiments was oriented perpendicular to the constant field) these additional resonators satisfy the selection rules for two-photon transitions. In addition, resonances were observed corresponding to transitions in which three and more photons participated. Later on, detailed theoretical and experimental investigations were made, concerning the observation of multiphoton resonances and the variation of their intensity, line width, and position of the resonant frequency with the amplitude of the rf field. (The influence of the intensity of the radio-frequency field on the width and position of the resonance line is manifest only at large amplitudes, and could not be obtained from the elementary perturbation theory developed in Chapter I, Sec. 2).

In the optical method of detection of multiphoton transitions, a check on formula (29) for the probability of the p-photon transition calls for establishment of a connection between the quantities S [expression (31)] and W(t). Such a connection is relatively simple, provided only the effects of the optical and radio frequencies are not correlated and can be regarded as independent. This condition is satisfied when the sodium atoms are oriented with light having approximately identical intensity of the D_1 and D_2 lines. In this case all the sublevels of the ground state decay at the same rate like $\exp(-\Gamma_1 t)$. Here Γ_1 is the relaxation width of the sublevels of the ground state, with $\Gamma_1 = 1/\tau + 1/T$, where τ is the average time between two collisions of the atom with the walls of the cell (the main relaxation mechanism), and T the average time between two acts of absorption of optical photons by each atom.

The considerable difficulty of comparing the experimental results with the theoretical ones is connected with the fact that S depends essentially on the degree of disorientation of the atoms in the excited state. On the other hand, the disorientation mechanism is not sufficiently well known, and the change of the distribution of the atoms over the sublevels of the ground state, caused by the disorientation, does not lend itself to a direct experimental or theoretical determination.

It will be convenient in what follows to consider separately two cases of polarization of the radio frequency field: a field rotating in a plane perpendicular to H_0, and a linearly oscillating field of arbitrary orientation.

2. Multiphoton processes in a rotating field. A theoretical analysis of multiphoton processes in a rotating field perpendicular to a uniform constant field H_0[26] leads to the following expression for the magnitude of the signal S, corresponding to the p-photon transition

$$S_{mn}^{(p)}=\frac{2\,|K_{mn}^{(p)}|^2}{(\omega_{nm}-p\omega)^2+\Gamma_1^2+4\,(1+\Delta_{mn}/2)\,|K_{mn}^{(p)}|^2}. \qquad (32)$$

Here $K_{mn}^{(p)}$—composite matrix element of the p-photon transition $m \to n$, ω_{nm}—frequency of the transition $m \to n$ (we assume henceforth that $\hbar = 1$), which generally speaking depends on the intensity of the rf field; ω—frequency of rf field, and Δ_{mn}—dimensionless parameter that depends on the degree of disorientation in the excited state and is generally speaking different for different transitions $m \to n$.

The form of the composite matrix element $K_{mn}^{(p)}$ depends, in accordance with (30), on the form of the interaction operator $\hat{V}$. For transitions between Zeeman sublevels of the ground state, having identical parity, $\hat{V}$ is the operator of magnetic dipole interaction. In the case of a magnetic field rotating with frequency ω,

$$H_1(t)=\mathbf{H}_1(\mathbf{i}\cos\omega t+\mathbf{j}\sin\omega t); \qquad (33)$$

the operator is $\hat{V} = -\mu H_1$, where μ—operator of dipole magnetic moment of the atom, and the matrix element $V_{ab} \neq 0$ only if $m_{F,a} - m_{F,b} = \pm 1$.* If the transition in which m increases by unity corresponds to absorption of one photon, then the transition in which m decreases by unity corresponds to emission of the same photon.

*We shall henceforth omit the subscript F of m_F.

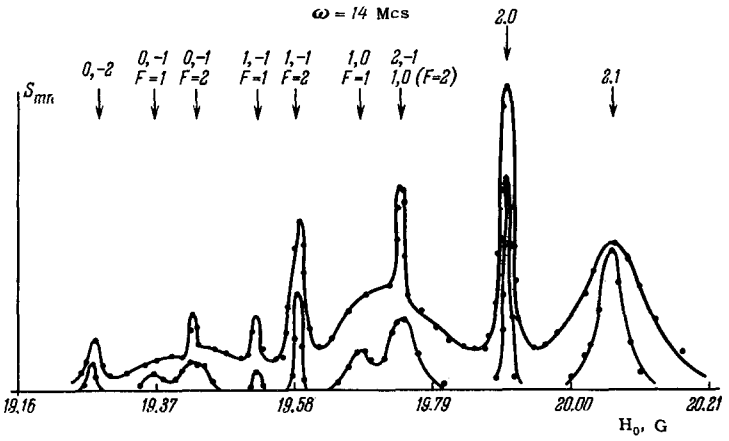

FIG. 7. Example of resonance spectrum observed in a rotating rf field.

A rotating magnetic field is equivalent to the presence of photons with only one polarization (for example σ^+). In such a field, transitions in which p-photons participate can occur only between the levels m and m ± p, that is, the order of the multiple-photon transition is uniquely determined by the change in the quantity m.

Although it is convenient to single out in the theoretical analysis the case of a rotating field, a linear oscillating field is always used in experiments. Such a field can be represented by a coherent superposition of right- and left-hand rotating fields with amplitudes $H_1/2$. Therefore, to investigate resonances, say, in a right-hand field it is necessary to produce conditions under which the influence of the left-hand field could be neglected. This influence decreases with increasing frequency ω and with decreasing field amplitude H_1. In this connection weak linearly-oscillating fields of relatively high frequency (4.95, 8.07, and 14 Mcs) were used to observe multiphoton transitions in a rotating field.

Figure 7 shows two typical spectra obtained for different amplitudes H_1. Resonances on the curve $S^{(p)}_{mn}(H_0)$ were observed at frequencies satisfying the condition $\omega_{nm} - p\omega = 0$. In weak fields, corresponding to the frequencies indicated above, the deviation from equidistant arrangement of the levels was ~10 kcs. This ensured sufficiently distinct separation of the individual resonances. At the same time, all the resonant frequencies lie close to the frequency of the single-photon transitions $\sim\omega_0$ between two neighboring sublevels.

The dependence of the intensity and width of the resonance lines on H_1 is determined by the composite matrix elements $K^{(p)}_{mn}$ in (32). The amplitudes of the resonances are obtained from (32) with $\omega_{nm} = p\omega$:

$$S^{(a)}_{mn} = \frac{2|K^{(p)}_{mn}|^2}{\Gamma_1^2 + 4|K^{(p)}_{mn}|^2(1+\Delta_{mn}/2)}. \qquad (34)$$

If H_1 is sufficiently small, such that $4|K^{(p)}_{mn}|^2(1+\Delta_{mn}/2) \ll \Gamma_1^2$, then the amplitude of the resonance of order p is proportional, in accordance with (30), to $|K^{(p)}_{mn}|^2 \sim (H_1)^{2p}$. Conversely, in sufficiently strong fields H_1, when $4|K^{(p)}_{mn}|^2(1+\Delta_{mn}/2) \gg \Gamma_1^2$, the amplitude of the resonance does not depend on the amplitude of the rf field (saturation effect). In the general case

$$S^{(a)}_{mn} = \frac{C_1 (H_1)^{2p}}{C_2 + (H_1)^{2p}}, \qquad (35)$$

where C_1 and C_2 are constants. Thus, theory predicts that the dependence of $(H_1)^{2p}/S^{(a)}_{mn}$ on $(H_1)^{2p}$ should be linear in all cases, $[(H_1)^{2p}/S^{(a)}_{mn} = a + b(H_1)^{2p}]$. As can be seen from Fig. 8, the experimental points for single-photon, two-photon, and three-photon transitions actually fall exactly on the straight lines.

The width of the resonance line of the p-photon transition is determined from (32):

$$\Delta\omega^{(p)}_{mn} = \frac{2}{p}\sqrt{\Gamma_1^2 + 4|K^{(p)}_{mn}|^2(1+\Delta_{mn}/2)}. \qquad (36)$$

Experimental investigations of the dependence of the width of the resonance lines on the amplitude H_1 of the rf field have shown that it is described satisfactorily not by formula (36), but by the expression

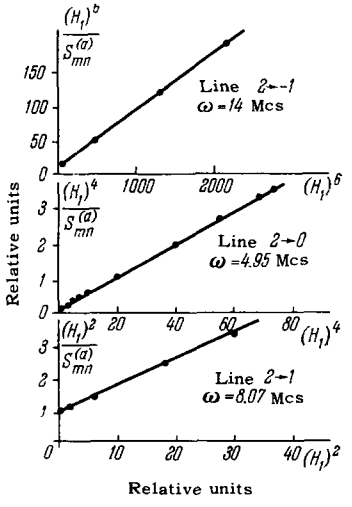

FIG. 8. Check of the equation $S_{mn}^{(a)} = (H_1)^{2p}/(b(H_1)^{2p} + a)$ for one-, two-, and three-photon transitions.

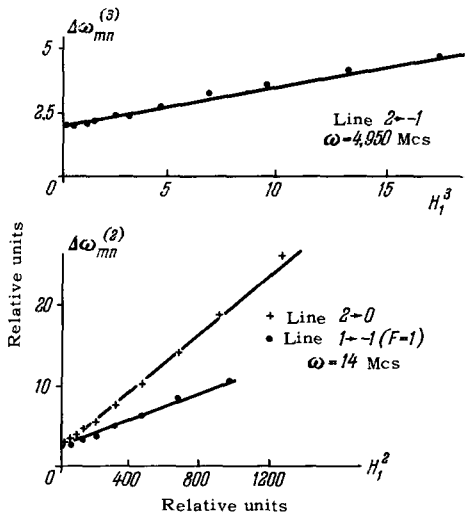

FIG. 9. Dependence of the line width of two- and three-photon transitions on the rf field amplitude.

$$\Delta\omega_{mn}^{(p)} = 2\left(\Gamma_2 + \frac{1}{p}\sqrt{\Gamma_1^2 + 4|K_{mn}^{(p)}|^2(1+\Delta_{mn}/2)}\right), \quad (37)$$

where $2\Gamma_2$—resonance line width due to inhomogeneity of the magnetic field H_0. Figure 9 shows the experimental dependences of the line widths of two- and three-photon transitions on H_1. The linear dependence $\Delta\omega_{mn}^{(p)} = f(H_1^p)$, except for very small H_1, denotes that the broadening by the rf field greatly exceeds the relaxation width $2\Gamma_1$. The intercept of the line on the $\Delta\omega_{mn}^{(p)}$ axis yields the direct inhomogeneous broadening $2\Gamma_2$, while the difference between the limiting width of the line at $H_1 \to 0$ and this value yields the relaxation width $2\Gamma_1$. An estimate of these quantities yields $2\Gamma_2 = 1.35$ kcs and $2\Gamma_1 = 400$ cps. To check the fact that Γ_2 is really due to the inhomogeneity of the field H_0, the limiting line widths of the one-, two-, and three-photon transitions were plotted against $\omega_0 = \gamma H_0$. Inasmuch as Γ_1 does not depend on the value of H_0, these dependences should be linear, as was indeed observed experimentally. Extrapolation to $\omega_0 = 0$ makes it possible to determine the quantity Γ_1, while the slope of the straight lines makes it possible to estimate the inhomogeneity of the field. Within the limits of the measurement accuracy, Γ_1 coincided with the quantity obtained from the relation $\Delta\omega_{mn}^{(p)} = f(H_1^p)$, while $\Delta H_0/H_0$ was of the order of 1/4000, in agreement with the result obtained from measurements by the method of proton nuclear resonance ($\Delta H_0/H_0 = 10^{-4}$).

It is of interest to compare the broadening of different lines by the radio-frequency field

$$\Delta\omega_{mn}^{*} = \frac{4|K_{mn}^{(p)}|}{p}\sqrt{1+\Delta_{mn}/2}. \quad (38)$$

The experimental value of the ratios $\Delta\omega_{mn}^{*}$ for two

Table I. Ratio of the broadenings of different lines by the field.

Frequency, Mcs	Broadening ratios considered	Theory	Experiment
4.95	$\frac{\Delta\omega^*_{2,1}}{\Delta\omega^*_{1,0\,(F=2)}}$	$\frac{K^{(1)}_{2,1}}{K^{(1)}_{1,0\,(F=2)}} = 0.8$	0.74
14	$\frac{\Delta\omega^*_{2,1}}{\Delta\omega^*_{1,0\,(F=2)}}$	$\frac{K^{(1)}_{2,1}}{K^{(1)}_{1,0\,(F=2)}} = 0.8$	0.91
14	$\frac{\Delta\omega^*_{2,1}}{\Delta\omega^*_{1,0\,(F=1)}}$	$\frac{K^{(1)}_{2,1}}{K^{(1)}_{1,0\,(F=1)}} = 1.4$	1.4
8.07	$\frac{\Delta\omega^*_{1,-1\,(F=2)}}{\Delta\omega^*_{2,0}}$	$\frac{K^{(2)}_{1,-1\,(F=2)}}{K^{(2)}_{2,0}} = 1.25$	1
8.07	$\frac{\Delta\omega^*_{2,0}}{\Delta\omega^*_{1,-1\,(F=1)}}$	$\frac{K^{(2)}_{2,0}}{K^{(2)}_{1,-1\,(F=1)}} = 2.4$	2.1
14	$\frac{\Delta\omega^*_{1,-1\,(F=2)}}{\Delta\omega^*_{2,0}}$	$\frac{K^{(2)}_{1,-1\,(F=2)}}{K^{(2)}_{2,0}} = 1.25$	1.1
14	$\frac{\Delta\omega^*_{2,0}}{\Delta\omega^*_{1,-1\,(F=1)}}$	$\frac{K^{(2)}_{2,0}}{K_{1,-1\,(F=1)}} = 2.4$	2.1
14	$\frac{\Delta\omega^*_{2,0}}{\Delta\omega^*_{0,-2}}$	$\frac{K^{(2)}_{2,0}}{K^{(2)}_{0,-2}} = 1$	1

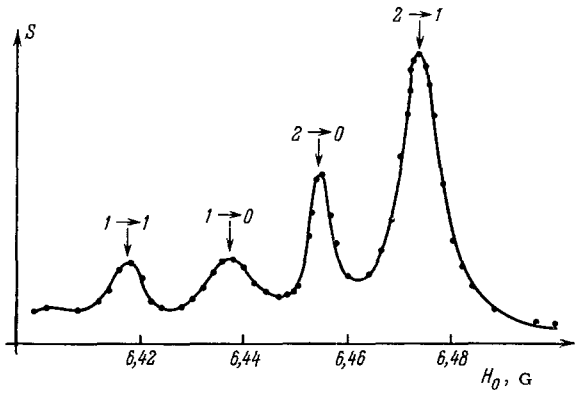

FIG. 10. Example of resonance spectrum for arbitrary orientation of the rf field in a plane perpendicular to the constant field H_0.

lines are determined from the slopes of the linear sections of the corresponding plots in the region $\Delta\omega_{mn} \gg 2(\Gamma_2 + \Gamma_1)$. Theoretical calculations of these ratios call for knowledge of Δ_{mn}, and were made under the assumption that Δ_{mn} does not depend on the levels of the transition $m \to n$. Table I lists the ratios of the values of $\Delta\omega^*_{mn}$ for some lines. The discrepancy between the theoretical and experimental values reaches 20%, apparently owing to the inaccuracy of the assumption Δ_{mn} = const.

3. Multiphoton transitions in a field of arbitrary orientation. A field of arbitrary orientation can be expressed in the form

$$\mathbf{H}_1(t) = \mathbf{i}H_x \cos\omega t + \mathbf{j}H_y \sin\omega t + \mathbf{k}H_z \cos(\omega t + \Phi), \qquad (39)$$

by suitably choosing the x and y axes. In the case when this field is perpendicular to the constant field H_0 ($H_Z = 0$), it can be represented by a superposition of two fields rotating in opposite directions and having amplitudes $H_+ = (H_X + H_Y)/2$ and $H_- = (H_X - H_Y)/2$:

$$\mathbf{H}_1(t) = H_+(\mathbf{i}\cos\omega t + \mathbf{j}\sin\omega t) + H_-(\mathbf{i}\cos\omega t - \mathbf{j}\sin\omega t). \qquad (40)$$

Therefore such a field is equivalent to the simultaneous presence of photons of both polarizations, σ^+ and σ^-. If the absorption of the photon σ^+ induces a transition $m \to m + 1$, and the emission induces a transition $m \to m - 1$, then the absorption of the photon σ^- induces the transition $m \to m - 1$, and emission induces the transition $m \to m + 1$. Accordingly, the interaction operator $V = -(\mu \cdot \mathbf{H}_1)$ has two types of matrix elements: $(\mu \cdot \mathbf{H}_1)^+ \sim (H_X + H_Y)$ and $(\mu \cdot \mathbf{H}_1)^- \sim (H_X - H_Y)$, so that transitions become possible, in which the change in Δm is not equal to the number of the photons participating in the elementary act. Thus, for example, the transition $\Delta m = 1$ can result from absorption of two σ^+ photons and one σ^-. This leads to the appearance of resonances of a new type, the frequencies of which coincide approximately with the odd harmonics of the one-photon resonances ω_0. The latter is connected with the fact that a change in the magnetic quantum number m by one can be effected only by using an odd number of photons. Now the composite matrix element $K_{mn}^{(p+q)}$, which includes, for example, the absorption of p photons σ^+ and q photons σ^-, will be proportional to $(H_X + H_Y)^p (H_X - H_Y)^q$.

A field with arbitrary polarization differs from the field just considered in the presence of a component parallel to the constant field H_0. This leads to the appearance of a new type of matrix element of the z-component of the interaction operator $\mu_Z H_Z$ [$(\mu_Z H_Z)_\pi$ and $(\mu_Z H_Z)^*_\pi$, which differ from zero only between states with identical value of m (with the exception of the case m = 0). The matrix element $(\mu_Z H_Z)_\pi$ corresponds to absorption, while $(\mu_Z H_Z)^*_\pi$ corresponds to emission of one photon with polarization π. In this connection, the presence of a longitudinal component of the rf field (π-photons) leads to the appearance of still another type of multiphoton resonance, namely resonances of even harmonics. Thus, for example, the resonance $\omega \approx \omega_0/2$ can correspond to the transition $m \to m + 1$ with participation of the photons σ^+ and π. The composite matrix element corresponding to the absorption of p-photons σ^+ and q-photons π will be proportional to $(H_X + H_Y)^p H_Z^q$. A distinguishing feature of transitions in which π-photons participate is that the intermediate states of the atom include also those between which the transition under consideration takes place.

Theory predicts a much lower probability for transitions with $\Delta m \neq p$ as compared with $\Delta m = p$. In the case when $\Delta m = p$ all the resonant frequencies $\omega \approx \omega_0$ and the energy differences in the denominators of the composite matrix elements are of the order of the deviation of the level spacing from equidistant, while for the transitions $\Delta m \neq p$ they are of the order of the energy of the single-photon transitions, that is, much larger. Therefore, to observe the resonances corresponding to $\Delta m \neq p$ it is necessary to go over to lower frequencies with larger rf field intensities.

Experimental studies were made of cases when the resonances with the even or odd harmonics of ω_0 in the transitions between different sublevels practically completely overlap or are still resolved.

Figure 10 shows an example of a spectrum observed in the region $\omega \approx \omega_0/2$ under conditions when the individual resonances are sufficiently resolved. The two resonances with $\Delta m = 1$ correspond to two-photon transitions, while the two resonances with $\Delta m = 2$ are due to four-photon transitions. An analysis of the spectra shows that the theoretically predicted dependences of the signal amplitudes and line widths on the amplitude of the rf fields are well satisfied. Figure 11a shows the results of a check on the law $(H_1)^6/S^{(a)}_{mn} = aH_1^6 + b$ for the three-photon transition $2 \to 1$ and of the investigation of the dependence of the width of the two-photon lines $2 \to 1$ and $1 \to 0$ ($F = 2$) on H_1^2 (Fig. 11b). The value obtained from these relations for the limiting width $2\Gamma_2 + \Gamma_1 = 1.65$ kcs is close to the value obtained in experiments with a rotating field. The

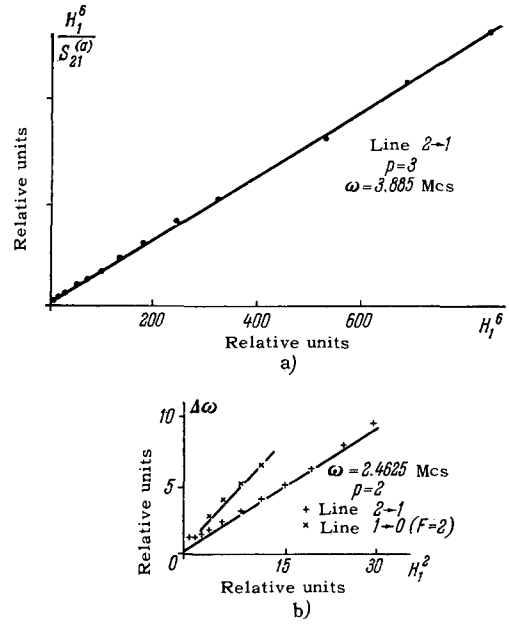

FIG. 11. Check of the equation $S_{mn}^{(a)} = (H_1)^{2p}/(a(H_1)^{2p} + b)$ for three-photon transition 2 → 1. b) Dependence of the width of the two-photon lines 2 → 1 and 1 → 0 (F = 2) on the rf field amplitude.

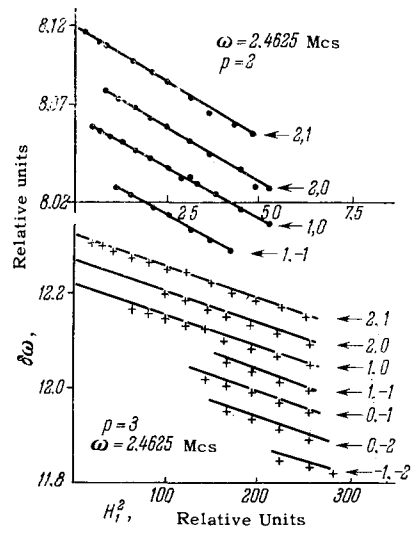

FIG. 12. Dependence of the shift of the resonant frequency of two- and three-photon transitions on the amplitude of the rf field.

widths of the four-photon lines were not investigated, since it was noted that for transitions with p > 3 the inaccuracy in their determination is very large as a result of the dependence of the resonant frequency on the power of the radio-frequency field. The latter is connected with the fact that the energy-level shift induced by the rf fields is not the same for different levels.

Quantum theory of multiphoton transition[14] considers the shift of the energy levels as a result of virtual emission and absorption of photons:

$$\Delta E_m = \sum_k \frac{V_{mk}V_{km}}{W_m - W_k}. \qquad (41)$$

(This relation is the usual expression for the change in the energy of the state m in second-order perturbation theory, and can be regarded as the diagonal element K^2_{mm} [see (30)].) In such virtual absorptions and emissions of photons, the atom has during the time interval when it is in the intermediate states an energy which is different from that of the initial unperturbed state, and this is manifest in an effective change in the energy of the initial state m. The shift of the level positions is usually much smaller than the widths of these levels in single-photon transitions. However, it can become quite appreciable for conditions of higher order. In the case considered here, that of four-proton transitions, the line broadening due to the rf field is of the order of $\mu^4 H_1^4/\omega^3$, and the shift of the resonant frequency is of the order $\mu H_1/\omega$ ($\hbar = 1$). When $\mu H_1 \ll \omega$, the shift of the resonant frequency turns out to be much larger than its width. Therefore a small change in the power of the rf field during the measurement process leads to a shift of the line by an amount exceeding its width.

The line shifts $\delta\omega$ were investigated for two-photon and three-photon transitions. Figure 12 shows the dependence of the position of these lines on H_1^2. In accord with the theory, they represent a set of parallel straight lines. A theoretical analysis gives for the ratio of the slopes of the two- and three-photon transitions a value of 1.78. The experimental values are 1.7 and 1.83 at field frequencies 2.4625 and 3.865 Mcs, and are in satisfactory agreement with the theoretical value.

As already noted, a certain difficulty in comparing the experimental and theoretical results is connected with the insufficiently accurate knowledge of the parameter Δ_{mn}. Above, in comparing the widths of the different lines, this parameter was assumed to be the same for transitions between arbitrary levels m and n. A crude theoretical estimate (without account of the nuclear spin) of Δ_{mn} for experimental conditions yields a value 1.2. On the other hand, to estimate the parameter Δ_{mn} we can use the fact that the broadening of the line by the rf field is determined by the quantity $K^{(p)}_{mn}$ and Δ_{mn}, and its displacement only by $K^{(p)}_{mn}$. Comparison for three-photon lines is given in Table II. The order of magnitude of the obtained values of Δ_{mn}

Table II

	$4\lvert K^{(3)}_{mn}\rvert$	$\Delta\omega^*_{mn}$	Δ_{mn}
2.4625 Mcs, Line 2—1	33	42	1.2
3.885 » » 2—1	18	24	1.6
3.885 » » 1—0(F=2)	22	25	0.6

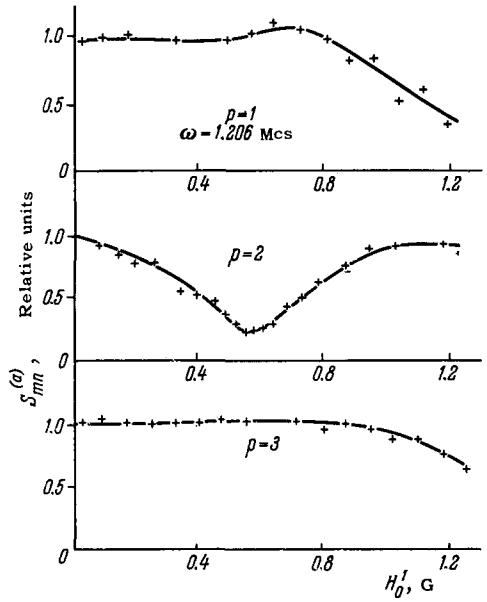

FIG. 13. Dependence of the intensities of resonances of one-, two-, and three-photon transitions on the degree of compensation of the perpendicular component of the constant field $H_0^{\perp}$ (the minimum of the two-photon transition intensity corresponds to the optimal compensation of this component).

corresponds to the theoretical one, but their scattering is sufficiently large. This leads to a relatively large (20%) inaccuracy in calculating the line widths from the observed shifts.

At the frequency 1.206 Mcs used in the present experiments, the different lines with nearly equal frequency are practically superimposed on one another, and only resonances of far frequencies, $\omega = \omega_0, \omega_0/2, \omega_0/3$, etc., can be resolved. The general dependences of the intensities of the resonances, line widths, and their shifts are the same as in the case of the resolved resonance. Theory predicts that resonances of even harmonics (for example, two-photon resonance) exist only if $(\mu_z H_z)_\pi \neq 0$, that is, if the projection of H_1 on the constant field H_0 does not vanish. A check on this prediction was made in the following fashion: the rf field was oriented approximately perpendicular to the constant field, after which a weak constant field H'_0 in the direction of the radio-frequency field was introduced (for example, along the Ox axis in Fig. 6). The change in the component H'_0 leads to a rotation of the total field, and at a certain value of H'_0 the longitudinal component of the radio-frequency field becomes equal to zero. Then the resonance of the two-photon transition should disappear, whereas the resonances of the single-photon and three-photon transitions should remain. The results obtained are shown in Fig. 13. The observed minimum of $S^{(2)}_{mn}$ for the two-photon resonance is not equal to zero because of the inhomogeneity of the radio-frequency and constant field over the entire volume of the cell.

The dependence of the quantity $S^{(2)}_{mn}$ on the presence of a longitudinal component of the radio-frequency field can be used to determine the direction of the constant magnetic field. If the rf field has sufficient homogeneity, then the signal of the two-photon transition is equal to zero when the constant field is perpendicular to the rf field, and appears when slight deviation from perpendicularity takes place. The accuracy with which the direction of the constant magnetic field is determined will depend on the minimum longitudinal component H_Z of the rf field which can still be observed at the available signal-to-noise ratio.

2. Two-Photon Absorption in the Optical Band

1. Two-photon absorption in $CaF_2:Eu^{++}$ crystals. The first time that two-photon absorption was observed in the optical band was in CaF_2 crystals activated with divalent europium Eu^{++}, replacing Ca^{++} ions[30]. Such crystals have an intense absorption band between 30,000 and 25,000 cm^{-1}, corresponding to electronic 4s—5d transitions of the Eu^{++} ions. When the crystals are excited with light in the same wavelength range, a bright blue fluorescence is observed with a bandwidth ~ 300 Å near 4200 Å. This fluorescence is interpreted as a result of nonradiative transition of Eu^{++} into an intermediate lower state with subsequent emission during a transition to the ground state. Since the lowest lying energy levels in the $CaF_2:Eu^{++}$ crystal correspond to an energy of 22,000 cm^{-1}, the crystals are transparent to the radiation from a ruby laser.

In the described experiments, the radiation from the ruby laser was focused on a thin (0.1 mm) slab of the $CaF_2:Eu^{++}$ crystal, located ahead of the entrance slit of a spectrograph. In front of the crystal were placed two red filters with transmission $< 10^{-4}$ for $\lambda < 6100$ Å, so as to exclude the possibility of blue or ultraviolet radiation from the pump lamp striking the crystal. The light passing through the crystal contained both the frequency of the incident laser emission and light with $\lambda = 4250$ Å, which was interpreted as a result of two-photon absorption. When inactivated crystals of CaF_2 were illuminated with a laser, no radiation with $\lambda = 4250$ Å was observed. It was found that the fluorescence intensity was proportional to the square of the laser-emission intensity, thus proving the two-photon absorption.

A rigorous calculation of the probability of two-photon excitation is at present impossible, for this necessitates knowledge of the structure of the energy bands of Eu^{++} in the CaF_2 crystal lattice, and of the matrix elements connecting the initial and final states with the intermediate states. A simplified analysis was given in[31], where it was assumed that the two-photon transition proceeds via one intermediate state, connected with the initial and final transitions with oscillator strength f, with the frequency corresponding to the position of this intermediate state being much

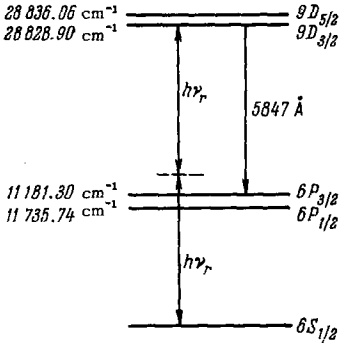

FIG. 14. Energy level scheme of the cesium atom.

higher than the frequency of the laser emission. The result was the following formula for the cross section of two-photon excitation:

$$\sigma_2 = \sigma_1 F, \quad \sigma_1 = \frac{r^2 \lambda_r^2 f}{n^2 \Delta\nu}, \tag{42}$$

where r = 2.8×10^{-13} cm is the classical radius of the electron, n—refractive index of the crystal, $\Delta\nu$—width of real excited state near double the laser frequency $2\nu_r$, and F—incident photon flux per cm^2 and per second. For $\lambda_r = 7 \times 10^{-5}$ cm, n = 1.4, $\Delta\nu = 1.5 \times 10^{14}$ sec^{-1}, and f = 1 this formula yields $\sigma_1 = 1.3 \times 10^{-48}$ cm^4 sec. The number of excitation acts per unit time in 1 cubic centimeter (at a quantum yield equal to unity), the number of emitted fluorescence photons is

$$N_{fl} = \sigma_2 N F, \tag{43}$$

where N—concentration of the impurity ions. In this experiment, the laser radiation (energy on the order of 0.1 J in a flash lasting 5×10^{-4} sec) was focused on an area of approximately 10^{-3} cm^2, corresponding to $F = 8 \times 10^{23}$ photons/cm^2 sec. Since the irradiated volume of the crystal was 10^{-4} cm^3, Eq. (43) yields 5×10^{10} fluorescence photons emitted per flash. This is in good agreement with the experimentally observed value.

2. Two-photon absorption in cesium vapor. Optical two-photon absorption in an atomic system was first observed upon excitation of cesium vapor with light from a ruby laser[32]. For two-photon absorption in a system with discrete energy levels, the energy of the transition to the excited level should be double the energy of the exciting photon, and the initial and final states should have the same parity. In cesium, transitions to the $9D_{5/2}$ and $9D_{3/2}$ levels correspond to energies 28,836.06 and 28,828.90 cm^{-1}, which is just close to double the energy of the ruby-laser photon (14,400 cm^{-1}), and their parity coincides with the parity of the ground state (Fig. 14). Inasmuch as the Doppler line width for these transitions, 0.04 cm^{-1}, is much smaller than the difference between double the laser photon energy and the transition energy, ~30 cm^{-1}, temperature tuning of the laser frequency was used to select the exact resonant frequency. Two-photon absorption was detected by observing fluorescence at a wavelength 5847 Å, corresponding to the spontaneous transitions $9D_{3/2} \rightarrow 6P_{3/2}$.

For such a simple atomic system as cesium, the probability of two-photon transition and the magnitude of the fluorescence signal can be calculated theoretically with a sufficient degree of accuracy. The main contribution to the two-photon absorption is made by the intermediate states $6P_{3/2}$ and $6P_{1/2}$, and the matrix elements corresponding to transitions to these states were calculated by the method proposed in[33].* It was expected that approximately 5×10^{12} atoms in a state $9D_{3/2}$ would be excited with a cesium vapor pressure 0.1 mm Hg and at a laser flash energy of 1 J. If we neglect the collisions of the cesium atoms, this would be accompanied by emission of 5×10^{11} photons with λ = 5847 Å.

The experimental setup was most elementary. The radiation from the ruby laser was focused on a cell with cesium vapor, in which the pressure could be varied over a wide range. The fluorescence light, filtered out with a $CuSO_4$ solution and with a narrow-band interference filter, was detected by a photomultiplier at right angle to the direction of the laser beam. The laser radiation passing through the cell split into two beams, one of which was guided to a second photomultiplier, and the other to the slit of a high-resolution spectrograph. Thus, both the fluorescence intensity and the wavelength and intensity of the laser radiation were registered simultaneously. It was established beforehand that in the absence of cesium vapor in the cell no fluorescence could be observed in the entire possible range of wavelengths of the laser. At a cesium vapor pressure 0.1 mm Hg, fluorescence was observed only if the central wavelength in the laser emission was equal to 6935.5 ± 0.05 Å. The dependence of the fluorescence on the wavelength of the laser emission in the presence of cesium vapor proves the presence of two-photon absorption.

The photoreceiver detected approximately 4×10^4 photons per pulse, which with account of the geometry and absorption by the filters corresponded to the emission of 5×10^9 photons, that is, two orders of magnitude lower than expected. The resultant disparity is connected, in the author's opinion, with the shortening of the lifetime of the Cs atoms in the $9D_{3/2}$ state, owing to nonradiative transitions to other levels upon collisions of the cesium atoms. Similar effects of extinction of the fluorescence of cesium vapor were observed earlier experimentally, and an estimate of their efficiency leads to a decrease in the fluorescence intensity by a factor of approximately 100, thus explaining the resultant disparity.

*At approximately the same time as this investigation, an article was published in which the oscillator strengths were calculated for cesium with account of the spin-orbit interaction[34].

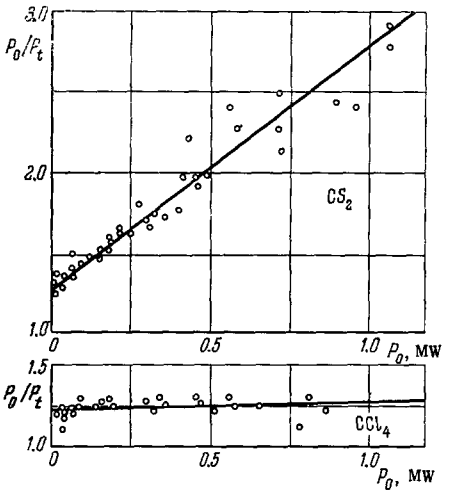

FIG. 15. Ratio of the exciting radiation power P_0 to the transmitted radiation P_2, vs. P_0, for CS_2 and CCl_4.

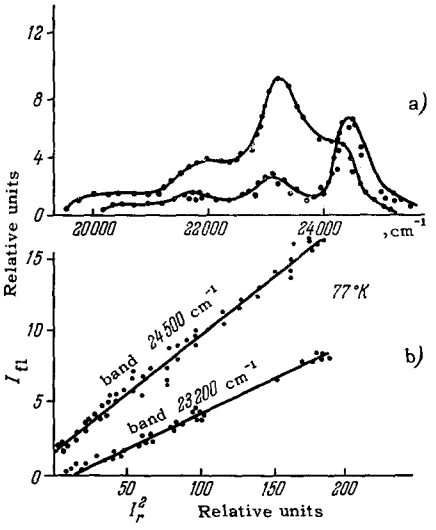

FIG. 16. a) Fluorescence spectrum of anthracene single crystals at 77 and 300°K, excited by a ruby laser. b) Intensity I_{fl} of the two principal maxima of fluorescence of anthracene crystals at 77°K against the intensity of the exciting laser radiation I_r (in arbitrary units).

3. Two-photon absorption in liquids that are active to Raman scattering. Two-photon absorption in liquids used to obtain stimulated Raman scattering was investigated in[35] (see Chapter III). Under ordinary conditions these liquids are transparent in the visible part of the spectrum, but two-photon absorption at high radiation density can lead to an appreciable loss of light and can hinder generation at the combination lines. To investigate this effect, a direct measurement was made of the absorption of the radiation from a ruby laser. A Q-switched laser was used, and to increase the radiation density the beam was focused on a cuvette with the liquid. The greatest peak power (P_0) in a pulse 4×10^{-8} sec in duration was 10^6 W at a spectral line width of 2 cm^{-1}. Figure 15 shows the dependence of the ratio of P_0 to the peak power P_t passing through the liquid, on P_0 for carbon disulfide (CS_2) and carbon tetrachloride (CCl_4) at room temperature. The errors are of the order of $\pm 30\%$ in the measurement of P_0 and 20% for P_0/P_t. The absorption of CCl_4 and a few other investigated liquids does not show any dependence on the flux F of the incident photons, thus showing the absence of two-photon processes. To the contrary, the absorption cross section σ of carbon disulfide depends linearly on the value of F and is described by the relation $\sigma = \sigma_0 + \sigma_1 F$, where $\sigma_1 = (5 \pm 4) \times 10^{-51}$ cm^4 sec. As can be seen from Fig. 15, when P_0 exceeds 0.5 MW the two-photon absorption of CS_2 exceeds the single-photon absorption.

The presence of relatively large two-photon absorption in CS_2 is related to the existence of an absorption band with $\Delta\nu \sim 10^{14}$ cps (due to the excited state $^1B_2$) in the vicinity of double the ruby-laser photon energy $2h\nu_r$. A theoretical estimate of the cross section of two-photon absorption by means of formula (42) with $\nu_r = 4.32 \times 10^{14}$ cps and f = 1 yields a value $\sigma_1 = 1.5 \times 10^{-48}$ cm^4 sec. The experimentally obtained value of σ_1 corresponds to an effective value f ~ 0.1.

4. Two-photon excitation of fluorescence in anthracene. Two-photon excitation of fluorescence in anthracene single crystals was observed in[36,37]. The light from a ruby laser was focused on slabs ranging in thickness from 100 μ to 2 mm, cut from single-crystal anthracene. The light passing through the slab was filtered with a $CuSO_4$ solution and focused after passing through a monochromator onto a calibrated photomultiplier. The signal from the resistance of the latter was fed to one of the inputs of a double-beam oscilloscope. The second input of the latter was a signal from a photoreceiver to which part of the laser radiation was diverted. To photograph the spectrum, the monochromator was replaced by a spectrograph with a grating.

In all the crystals, fluorescence excited by the laser radiation was observed at temperatures 300 and 77°K. Its spectrum (Fig. 16a) coincides with the spectrum of the fluorescence excited by radiation with wavelength larger than 3800 Å and corresponding to transitions from the excited $^1B_{2u}$ to the ground ^1A_g state. The quadratic dependence of the intensity of fluorescence on the intensity of laser radiation (Fig. 16b) can serve as an argument in favor of the two-photon mechanism of excitation of anthracene. A transition takes place here from the ground singlet to the first excited (also singlet) state with energy close to 28,800 cm^{-1}. In the case of single-photon excitation this state was not observed, owing to the equal parity with the ground state, but its existence was predicted theoretically.

It was observed subsequently that the maximum of the intensity of blue fluorescence of anthracene is delayed relative to the ruby-laser radiation pulse by a

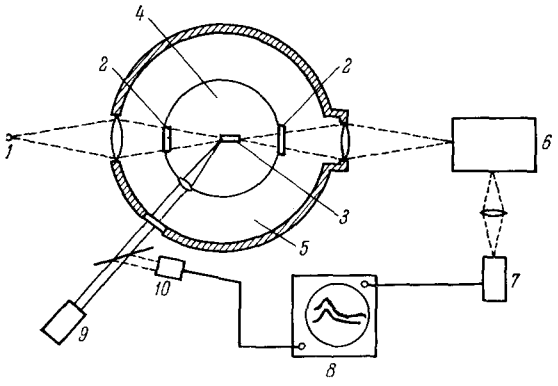

FIG. 17. Diagram of experimental set-up for the investigation of two-photon absorption spectrum in KI crystals. 1 – Xenon arc lamp, 2 – quartz window, 3 – sample, 4 – helium gas, 5 – vacuum, 6 – monochromator, 7 – photomultiplier for the ultraviolet region of the spectrum, 8 – double beam oscilloscope, 9 – ruby laser, 10 – photocell.

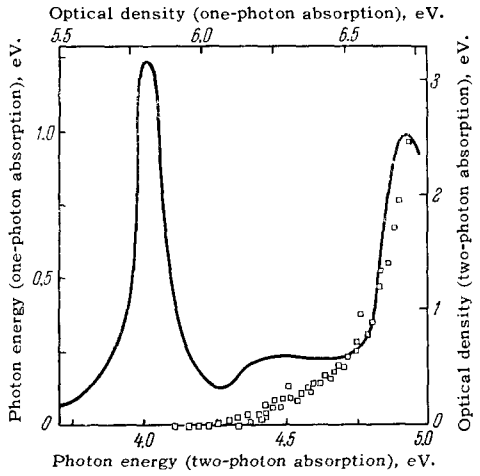

FIG. 18. Spectra of one- and two-photon absorption of KI crystals. Abscissas correspond to a ruby-laser photon energy 1.79 ev. ——— spectrum of one-photon absorption; □ – two-photon absorption spectrum.

time up to 4×10^{-2} sec[38]. In this connection, the hypothesis was advanced that there exists an intermediate (exciton) mechanism of fluorescence excitation, including recombination of two excitons with energy 1.8 eV and formation of an exciton with energy sufficient for the excitation of the luminescence of the anthracene. Experiments using a Q-switched ruby laser delivering radiation pulses of 3 MW power and of 3×10^{-8} sec duration have made it possible to observe two types of anthracene fluorescence—"undelayed," due to two-photon absorption, and "delayed," which is in good agreement with the notion of the exciton excitation mechanism[39]. The use of a laser with additional frequency transformation with the aid of Raman scattering has made it possible to trace the dependence of the anthracene fluorescence intensity on the wavelength of the exciting light. It was found that, accurate to 50%, the efficiency of two-photon excitation remains constant on going from λ = 6,943 Å to λ = 7,670 Å, whereas the efficiency of excitation in which the exciton mechanism participates decreases by an approximate factor of 5. This is evidence that two-photon absorption in anthracene has a nonresonant character, and absorption with formation of excitons is a resonant process.

5. Investigation of the spectrum of two-photon absorption in KI crystals. In this experiment[40] two-photon absorption in KI crystals was observed for the first time, using a ruby laser and a source of ultraviolet radiation with continuous spectrum. This has made it possible to investigate the spectrum of two-photon absorption near the edge of the main absorption band of the crystal and to obtain additional information on the nature of the excited states. Because of the low value of the two-photon absorption compared with single-photon absorption in the region of the absorption band, it became possible to change from layers with thickness on the order of several microns to large-size crystals, which is an important advantage of the employed procedure over investigations of single-photon absorption.

A diagram of the experimental set-up is shown in Fig. 17 (several light filters have been left out from the figure). The pulsed energy of the laser was approximately 15 J; the sample measured 2 × 3 × 25 mm. A measure of the two-photon absorption was the decrease in a xenon-lamp radiation transmitted through the sample under the action of the laser pulse (the greatest change in the intensity was approximately 0.2%). Oscillograms of the laser pulse and of the signal due to the change in the absorption were similar in shape, thus indicating that the two-photon absorption is proportional to the intensity of the laser emission.

Figure 18 shows the spectrum of single-photon absorption of a thin layer of KI[41] at −180°C, and the two-photon absorption spectrum obtained in the same investigation with the crystal at liquid-helium temperature (the temperature shift is 0.05 eV).

The single-photon absorption bands are usually identified with excitons, for which three models were proposed[42]. In the first model the exciton is defined as an excited state of the halide ion (3P—4S transition), in the second as an excited state with transfer of one of the 3P electrons of the halide ion to the state 3S of the six metal ions surrounding the halide ion, and in the third the excitation is ascribed to many cells of the crystal lattice. The most interesting feature of the two-photon absorption spectrum is that it does not contain any bands corresponding to the total energy of the laser photon and the xenon-lamp photon, which is equal to 5.8 eV. This means that the 5.8 eV absorption band does not have states with parity coinciding with the parity of the ground state. This condition is

not satisfied by the charge-transfer model. The relatively high level of fluctuation noise does not permit more definite conclusions to be drawn from the experiments in question.

III. MULTIPLE PHOTON PROCESSES REQUIRING AN ACCOUNT OF INTERFERENCE PHENOMENA

1. General Remarks

In many multiple-photon processes, there occur interference phenomena and the system cannot be described exclusively in terms of the populations of the individual states and the photon numbers. The interference phenomena are observed in the case when the path of transition of the system from the initial to the final state is not unique, and have a simple physical meaning: reliable knowledge of the initial and final states of the system is not sufficient to indicate the path along which the system has gone over from one state to the other. An example of this was given above (see Chapter I, Sec. 2) in the discussion of two-photon absorption, where the ambiguity of the transition was connected with the fact that it is impossible in principle to indicate the sequence in which the photons are absorbed. Another example, which will be considered below, can be the process of generation of harmonics. Its efficiency depends essentially on the phase relations between the waves scattered by different centers.

The main features of the interference phenomena of interest to us can be demonstrated using as an example the resonance fluorescence of an ensemble of noninteracting atoms, the levels of which can, generally speaking, be degenerate. Two possible types of interference phenomena are possible in this case. These are the interference phenomena which occur in the elementary act of scattering by each of the isolated atoms, and the interference phenomena connected with the specific nature of the scattering by the entire aggregate of atoms. Effects connected with the interference phenomena of the former type will be observed even when the scattering system consists of only one atom; on the other hand, effects of the second type will be missing in such a case. The main features of the interference phenomena of the first type can be explained by considering the scattering of a single photon by an atom having a k-fold degenerate excited level n (simultaneous degeneracy of the lower level, too, does not lead in principle to new results). In this case the final state of the system (atom at the ground level, photon ω_ρ absorbed and photon ω_σ emitted) can be attained in k different ways $m \to n_k \to m$ (we assume that the probabilities of all the paths, defined by the corresponding matrix elements, are equal or comparable). This causes the probability of the elementary act of the resonance fluorescence to be given now not by formula (24), but by the relation [see[17], formula (52)]

$$W_{\rho\sigma} = \frac{1}{\hbar^4}\left|\sum_k \frac{V^{(\rho)}_{mn_k} V^{(\sigma)}_{n_k m}}{[i\gamma_m + \omega_\rho - \omega_\sigma]\,[i\gamma_{n_k} + \omega_\sigma - \omega_{n_k m}]}\right|^2. \tag{44}$$

It is seen from this expression that it is not the probabilities of transitions along different paths that are additive, but their amplitudes, and this leads to the occurrence of "probability interference." This interference disappears only if the degeneracy is lifted and the distances between the sublevels n_k become appreciably higher than the natural width γ_{nk}. Then, as can be readily seen from (44), there is no final state that can be reached with equal probability via many paths. In Sec. 2 of this chapter we describe the experimentally observed effects resulting from the presence of probability interference in the elementary act of scattering of a photon by an individual atom. In these experiments, the transition to scattering by an aggregate of N noninteracting atoms is made by simply adding the probabilities of scattering by each of the N atoms (that is, a simple increase of the scattering effect by a factor N).

Interference phenomena of the second type, connected with the scattering of a photon by an ensemble of identical atoms, which for simplicity are assumed to have nondegenerate levels, are due to the possibility in principle of the photon being scattered by any of the N atoms. If we cannot indicate the precise atom from which the photon is scattered, this means that there are N possible paths for the system to go from the initial to the final states. Therefore the ensemble of N identical atoms with nondegenerate levels m and n can be regarded as a system with N-fold degenerate intermediate state. In each of these there is absorbed a photon ω_ρ and one of the atoms is excited, while the remaining N − 1 atoms remain in the ground state. Unlike the case considered above, that of one atom with degenerate excited state, in a system of N atoms it is necessary to take into account the difference in the positions of the scattering atoms. This can be done by taking into consideration the coordinate dependence of the matrix elements $V^{(\rho)}_{mn}$ and $V^{(\sigma)}_{nm}$, which we have neglected above. It follows from quantum theory that the matrix element $V^{(\rho)}_{mn}$ for the absorption of a photon ω_ρ with momentum $\mathbf{k}_\rho$ by an atom situated at the point with coordinate $\mathbf{R}$, contains a factor of the form $\exp(-i\mathbf{k}_\rho \cdot \mathbf{R})$, and the corresponding matrix element $V^{(\sigma)}_{nm}$ for the emission of a photon ω_σ with momentum $\mathbf{k}_\sigma$ contains a factor $\exp(i\mathbf{k}_\sigma \cdot \mathbf{R})$. Therefore the composite matrix element for the scattering by a single atom, corresponding to the absorption of a photon with momentum $\mathbf{k}_\rho$ and emission of a photon with momentum $\mathbf{k}_\sigma$, can be written in the form

$$K^{(2)}_{\rho\sigma} = A_{\rho\sigma} \exp[-i(\mathbf{k}_\rho - \mathbf{k}_\sigma)\mathbf{R}], \tag{44'}$$

with $A_{\rho\sigma}$ including all the factors which do not depend on the coordinate $\mathbf{R}$. An examination of the result of the scattering of all N atoms is in general a very complicated problem. However, as shown in[17], in the

two particular cases which will be considered below, and which correspond to conditions under which the scattering of the photon by each of the atoms of the ensemble is independent, the composite matrix elements for the scattering by an aggregate of N identical atoms $K_N^{(2)}$ is the sum of the composite matrix elements for the scattering by the individual atoms:

$$K_N^{(2)} = A_{\rho\sigma} \sum_{i=1}^{N} e^{-i(\mathbf{k}_\rho - \mathbf{k}_\sigma)\mathbf{R}_i}, \tag{45}$$

where R_i—coordinate of the i-th atom. Inasmuch as the probability of scattering is proportional to the square of the modulus of this matrix element, the expression for the scattering intensity contains interference terms. Indeed, $|K_N^{(2)}|^2$ will contain terms of the form

$$2\{1 + \cos[(\mathbf{k}_\rho - \mathbf{k}_\sigma)(\mathbf{R}_{k'} - \mathbf{R}_{k''})]\}, \tag{46}$$

in which the product $(\mathbf{k}_\rho - \mathbf{k}_\sigma)(\mathbf{R}_{k'} - \mathbf{R}_{k''})$ is the path difference (that is, the phase difference) of the waves scattered by the atom with coordinate $\mathbf{R}_{k''}$ and the atom with coordinate $\mathbf{R}_{k'}$, expressed in units of λ. The result of the scattering by any pair of atoms of the ensemble depends essentially on the value of this product. In particular, if it is a multiple of 2π, then the intensity of scattering by two atoms exceeds by a factor of 4 the intensity of scattering by a single atom. We shall demonstrate the result of taking into account all N atoms of the ensemble by means of two particular cases, which are of interest in what follows.

Let us assume that all N atoms are concentrated in a volume with linear dimensions that are smaller than the wavelength λ (this case can be readily realized in the radio band). Then $(\mathbf{k}_\rho - \mathbf{k}_\sigma)(\mathbf{R}_{k'} - \mathbf{R}_{k''}) < 1$, and all the exponentials in (45) are replaced by unities, so that the total probability of scattering is proportional to N^2. If $N \gg 1$, this interference effect leads to a large increase in the probability of the elementary scattering act, compared with incoherent scattering proportional to the number of atoms N. It is immaterial here whether the frequency of the scattered radiation lies within the natural line width γ_{mn} corresponding to the transition $m \to n$, or outside it.

Let us assume now that the linear dimensions of the region occupied by the ensemble of atoms are considerably larger than the wavelength, and the frequency of the exciting radiation lies outside γ_{mn} (nonresonant scattering). It is shown in [17] that in this case the total intensity of the scattering is also determined by formula (45), and there is no phase difference between the incident and scattered radiations. We shall henceforth be interested in one special case of nonresonant scattering—generation of a second harmonic in the optical band. The elementary act of this process consists in the absorption of two photons with momentum $\mathbf{k}_1$ and emission of a single photon with momentum $\mathbf{k}_2$. Generalization of (45) to include this case yields for the composite matrix element an expression

$$K_N^{(3)} = \text{const} \cdot \sum_{i=1}^{N} e^{-i(2\mathbf{k}_1 - \mathbf{k}_2)\mathbf{R}_i}. \tag{47}$$

We shall use this expression to consider an ensemble consisting of N atoms spaced distances a apart on the x axis, the length of the chain being $l = Na \gg \lambda$. Assuming that radiation with wavelength λ propagates along the x axis, we find that the intensity of radiation of doubled frequency, propagating in the same direction, is

$$I_2 = \text{const} \left| \sum_{n=1}^{N} e^{i(2k_1 - k_2)an} \right|^2 = \text{const} \cdot \frac{\sin^2 l(2k_1 - k_2)/2}{\sin^2 a(2k_1 - k_2)/2}. \tag{48}$$

In the case when $a \ll l$ but $l(2k_1 - k_2)/2 \geq \pi$, we can replace $\sin^2 a(2k_1 - k_2)/2$ by $a^2(2k_1 - k_2)^2/4$ and

$$I_2 = \text{const} \cdot \frac{\sin^2 \frac{l}{2}(2k_1 - k_2)}{(2k_1 - k_2)^2}. \tag{49}$$

When $l(2k_1 - k_2)/2 \ll 1$ the efficiency of generation of the second harmonic in the x direction should be proportional to the square of the length of the chain l, or to the square of the scattering atoms N. It will be shown in Sec. 3 of the present chapter that this effect is of great importance for the generation of optical harmonics.

2. Processes Connected with Interference Phenomena in Each of the Atoms of the Ensemble

1. Effect of "level crossing." In 1959, in experiments on the observation of resonant fluorescence of helium atoms (transition $2^3S_1 - 2^3P$) in a magnetic field oriented perpendicular to the direction of propagation of the exciting light, it was observed that the intensity of the scattered light increases sharply for definite values of the magnetic field intensity [55,56]. These resonant values of the magnetic field corresponded to energies at which the different sublevels of the fine structure of the excited state 2^3P cross, as a result of which the effect was called the "level crossing" effect. Figure 19 shows the energy scheme of the ^3P and $^3S_1$ states of the helium atoms in a magnetic field, with the circles denoting the points of the crossing of the levels, leading to an abrupt change in the scattering intensity.

The "level crossing" effect can be described in simplest fashion in terms of the "probability interference" of the elementary act of scattering of the photon by each of the scattering atoms of the ensemble. For simplicity we shall assume that the scattering atom has in the excited state two sublevels n_1 and n_2 ($E_{n_2} > E_{n_1}$) with half widths $\gamma_{n_1} = \gamma_{n_2} = \gamma$, and the ground state m is not degenerate. Then, according to (44), the resonance scattering probability is

$$W_{\rho\sigma} = \frac{1}{\hbar^4[(\omega_\rho - \omega_\sigma)^2 + \gamma_m^2]} \left| \frac{V_{mn_1}^{(\rho)} V_{n_1 m}^{(\sigma)}}{\omega_\sigma - \omega_{n_1 m} + i\gamma} + \frac{V_{mn_2}^{(\rho)} V_{n_2 m}^{(\sigma)}}{\omega_\sigma - \omega_{n_2 m} + i\gamma} \right|^2. \tag{50}$$

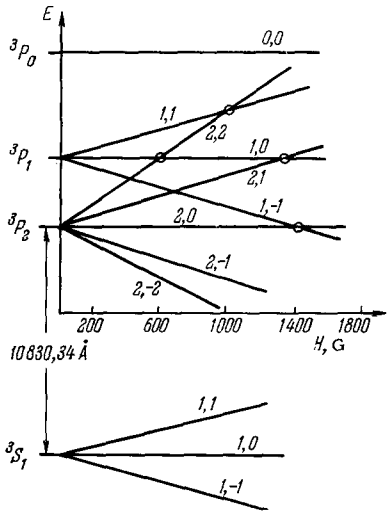

FIG. 19. Energy level scheme of ^3P and $^3S_1$ states of the helium atom in a magnetic field. The circles denote level crossings, which lead to a sharp decrease in the scattered light intensity.

Assuming that within the limits of the excitation line width γ the spectral density of the scattered radiation is constant (this condition was satisfied in the experiment in question), we obtain as a result of integration of (50) with respect to ω_ρ and ω_σ the total intensity of scattering of light in the form

$$I = \text{const} \cdot \left\{ \frac{|V^{(\rho)}_{mn_1}|^2 |V^{(\sigma)}_{n_1 m}|^2}{\gamma} + \frac{|V^{(\rho)}_{mn_2}|^2 |V^{(\sigma)}_{n_2 m}|^2}{\gamma} + \frac{4\gamma (A + A^*)}{4\gamma^2 + (\omega_{n_2} - \omega_{n_1})^2} + i \frac{2(A - A^*)(\omega_{n_2} - \omega_{n_1})}{4\gamma^2 + (\omega_{n_2} - \omega_{n_1})^2} \right\}, \quad (51)$$

where

$$A = V^{(\rho)}_{mn_1} V^{(\rho)*}_{mn_2} V^{(\sigma)}_{n_1 m} V^{(\sigma)*}_{n_2 m}.$$

If the levels do not cross, namely $(\omega_{n_2} - \omega_{n_1}) \gg \gamma$, then an appreciable contribution to the intensity of the scattered light is made only by the first two terms, which describe the result of independent scattering of the light via the intermediate states n_1 and n_2. Each of the sublevels n_1 and n_2 of the excited state scatters effectively only the harmonics which lie in a frequency band of width γ near ω_{n_1} and ω_{n_2} respectively. The result of such an independent scattering is determined by the squares of the moduli of the matrix elements V_{mn_1} and V_{mn_2}, and does not depend on the ratio of the phases of the scattered light. On the other hand, when the difference $\omega_{n_2} - \omega_{n_1}$ becomes comparable with the width of the sublevels, an appreciable role can be played by the interference terms, which describe the effect of scattering of each harmonic of the light simultaneously by both sublevels n_1 and n_2. It is the appearance of this interference scattering which leads to a sharp change in the intensity of the scattered light. As expected, for this we must have $V^{(\rho)}_{mn_1} \neq 0$ and $V^{(\rho)}_{mn_2} \neq 0$, that is, the excitation of both sublevel n_1 and n_2 from the common ground level must be allowed by the selection rules. The interference of different harmonics makes no contribution to the interference scattering, inasmuch as the interference contribution from the different harmonics depends on the phase relations between the harmonics (the phase factors of the corresponding harmonics enter into the matrix elements $V^{(\rho)}_{mn_1}$ and $V^{(\rho)}_{mn_2}$), and is equal to zero when the phases of the different harmonics are randomly distributed.

The effect of "level crossing" was used immediately after its discovery as a method for measuring the lifetimes and the structure of the excited atomic states[57-59]. The width of the region of the magnetic field at which a resonant change in the intensity of the scattered light is observed determines directly the lifetimes of the investigated states. The most important feature of such a method of determining the lifetimes of excited atomic states lies in the fact that this determination can be made under conditions when the inhomogeneous linewidth of excitation (for example, the Doppler width) can exceed by several orders of magnitude the natural line width for the excitation of a single atom. The absolute value of the magnetic field intensity corresponding to the level crossing can be used to determine the fine or hyperfine splitting constants.

We note that Hanle's experiments on the investigation of the polarization of resonant fluorescence in a magnetic field can be regarded as a particular case of the effect of "level crossing" in a zero magnetic field.

2. Effect of "parametric resonance." A new phenomenon which can be classified as multiple-photon, connected with the interference processes in each isolated atom of the ensemble, was observed in[60,61]. This phenomenon, called "parametric resonance," consists in the modulation of the intensity of the resonant fluorescence of atoms which have in the excited state a system of closely lying sublevels, if the frequency of the transition between the latter (the parameter of the system) coincides with or is a multiple of the frequency of an external magnetic field of definite orientation.

A block diagram of the set-up[60] used to observe this phenomenon is shown in Fig. 20b. Linearly polarized light from a cadmium lamp excites resonant fluorescence in cadmium vapor (transition $5^3P_1 - 5^1S_0$, $\lambda = 3261$ Å), kept at a temperature 200°C in a vessel shaped like a Wood's horn. The excited light propagates along a constant magnetic field H_0, produced by a system of Helmholtz rings, so that the level with $m = 0$ of the state 5^3P_1 (Fig. 20a) is not excited. The resonant fluorescence is registered by an FÉU-46A photoelectronic multiplier at some angle (in particular, right angle) to the direction of H_0. Since the line width of the radiation of the cadmium lamp is larger than the line width of the absorption of cadmium vapor, each of the sublevels with $m = 1$ and $m = -1$ can be excited

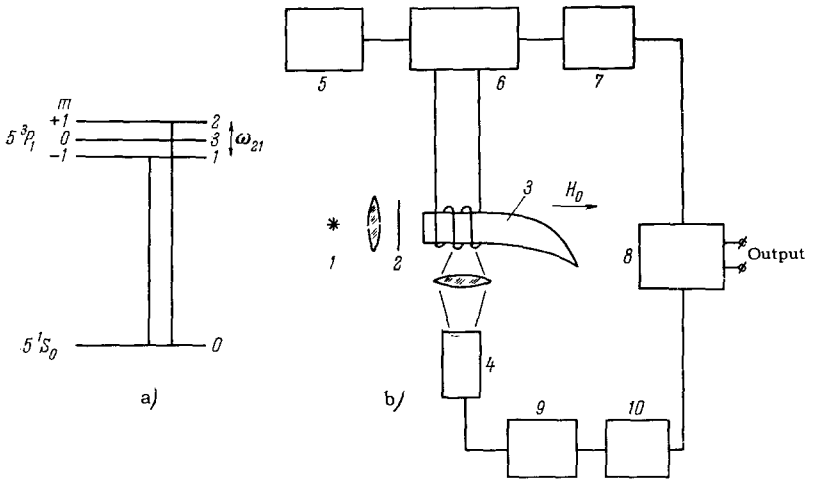

FIG. 20. a) Resonance level scheme of cadmium. b) Block diagram of experimental set-up for the observation of the "parametric resonance" effect. 1 – Cadmium lamp; 2 – linear polarizer; 3 – vessel with vapor; 4 – photomultiplier; 5 – GSS-6 standard signal generator; 6 – power amplifier; 7 – ZG-12 audio generator; 8 – synchronous detector; 9 – amplifier; 10 – detector.

with practically equal intensity. However, no effects of modulation fluorescence (interference of transition probabilities) was observed, inasmuch as the excitation of each of the sublevels is connected with different harmonics ($\omega_{21} \gg \gamma$). The situation is different if an alternating magnetic field of frequency Ω, polarized along the constant magnetic field H_0, is applied to the system with the aid of a solenoid placed over the horn. Under these conditions the intensity of the scattered light is modulated with frequency Ω and its multiple frequencies, and sharply pronounced resonance phenomena are observed if the frequency of the transition between the sublevels ω_{21} approaches Ω or one of its multiples.

Leaving aside a theoretical analysis of the parametric resonance phenomenon, given in[60,62], we note that it can be interpreted as a multiphoton process in which the scattering of each photon of plane-polarized radiation with energy corresponding to the transition from the sublevel from m = 1 or m = − 1 can occur, in the presence of an alternating magnetic field with frequency $\Omega = \omega_{21}/k$, (k—integer), in two ways in each atom. To explain this, let us consider one of the harmonics of the exciting radiation, which is in resonance with the transition to one of the sublevels (for example, m = − 1). By virtue of the linear polarization, this harmonic could excite also a transition to the second sublevel (with m = 1), but its energy is too small for this purpose (we assume that $\omega_{21} \gg \gamma$). Consequently, the photons will be scattered only by one sublevel. On the other hand, in the presence of a radio-frequency field the additional energy necessary for the excitation to the second sublevel can be acquired by the atom by absorbing simultaneously one photon of the harmonic in question and one photon from the radio-frequency field $\Omega = \omega_{21}$. As a result it turns out that both states of the atom are excited by the same optical harmonic, that is, the scattering of the optical photon can occur along two paths, as a result of which interference of the probabilities takes place. The phase difference of the waves scattered along these paths is determined here by the radio-frequency field. Since this field is coherent, this phase difference turns out to be the same for all atoms of the ensemble, making it possible to observe modulation of the scattered radiation.

In perfect analogy, a photon with frequency corresponding to the transition to the sublevel with m = + 1 can be scattered both directly via this sublevel and via the sublevel with m = − 1, with simultaneous stimulated emission of a radio-frequency photon, if $\omega_{21} = \Omega$. Scattering via two sublevels can occur also with absorption or stimulated emission of several radio-frequency photons, that is, at $\Omega = \omega_{21}/k$. Inasmuch as the radio-frequency field enters into the scattering probability amplitude only via one of the excited states, it is obvious that the dependence of the depth of modulation of the scattered light on the amplitude H_1 should be linear when $\Omega = \omega_{21}$, quadratic when $\Omega = \omega_{21}/2$, etc., as was indeed confirmed experimentally.

The region of frequencies Ω (or ω_{21} if Ω = const) within which a transition via two sublevels is observed is determined by the value of γ, and observation of resonances in the scattering of light can be used to determine the lifetime of the excited state. The lifetime of the excited state of Cd obtained in this manner, $\tau = 2.4 \times 10^{-6}$ sec, is in good agreement with the previous well-known value of this quantity for cadmium.

It was assumed above that the splitting is sufficiently large and $\omega_{21} \gg \gamma$. On the other hand, if $\omega_{21} \ll \gamma$ (zero splitting), then the scattering of photons with frequency $\omega \approx \omega_{10} \approx \omega_{20}$ is possible simultaneously via the two sublevels, without participation of the radio-frequency field (the "level crossing" effect). It is remarkable that superposition of a radio-frequency field leads in this case also to modulation of the intensity of the scattered light, the depth of which decreases with increasing Ω. This phenomenon can also be interpreted within the framework of the notions of scattering-probability interference, for which two

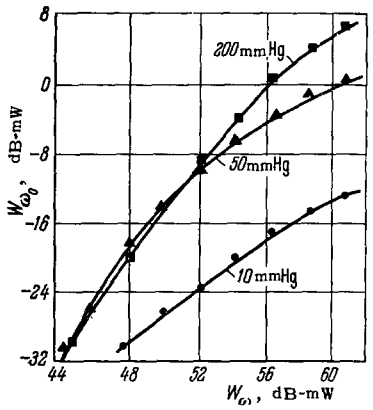

FIG. 21. Experimental dependence of the third-harmonic signal power at the output of the resonator on the magnetron excitation power for different pressures of the ammonia gas.

possibilities exist. The first corresponds to the excitation of the atom either directly by the optical photon or by the same photon with simultaneous absorption of one radio-frequency photon; the second corresponds to excitation of the atom either directly by the optical photon or by the same photon with simultaneous stimulated emission of one radio-frequency photon. Either possibility of probability interference corresponds to simultaneous emission of two harmonics, the frequencies of which differ by Ω. The theory of the phenomenon predicts that the depth of modulation of the scattered light will depend on the angle of observation Φ relative to the direction of the field H_0 like $I \sim \cos^2\Phi$, a dependence which was confirmed experimentally.

3. Multiphoton Processes Connected with Interference Phenomena in an Ensemble of Non-interacting Systems

1. Generation of harmonics in the centimeter band. The possibility of generation of harmonics in the centimeter band via a multiple-photon process was first demonstrated by an example wherein an electric dipole transition was excited in ammonia molecules, corresponding to the frequency ω_0 = 23,870 Mcs[67-69]. Ammonia gas in thermodynamic equilibrium filled a flow-through resonator having two resonant frequencies that differed by a factor of 3. Generation was observed at a frequency close to ω_0 when the resonator was excited by a pulsed magnetron operating at a frequency ω that was lower by one-third. Owing to the level shift of the investigated transition in the ammonia, the generated frequency was shifted under the influence of the exciting field by an amount on the order of 0.1 ω_0, and therefore the resonator was tuned to the frequencies 25,560 and 8,520 Mcs.

The experimental dependences of the power of the third harmonic on the excitation power for different ammonia pressures are shown in Fig. 21. At the maximum excitation power $W_\omega \sim 1$ kW, the output power was of the order of 10—30 milliwatts (theoretical calculations have shown that it can be raised to several watts[67]). Near the initial portions of the curves plotted at high pressures, $W_{\omega_0} \sim W_\omega^3$, which agrees with the theoretical predictions. Deviation from this law with increase in excitation power is connected with the fact that as the populations of both levels become equalized, the magnitude of the absorbed power decreases, and with it the generated power. It can be shown that in the limit, when the populations of the lower and upper levels become equal, there will be no frequency conversion at all. The deviation from cubic dependence at low pressures is due to the nonuniformity of the exciting field in the resonator, which leads to different frequency shifts at different points and to a change of the fraction of the resonator volume in which the effective frequency conversion takes place, with changing radiation power. At large pressures, this effect does not come into play, inasmuch as the absorption line width becomes so large that the working volume becomes practically independent of the power of the exciting field.

The high efficiency of the conversion of the field energy with frequency ω into the third harmonic (on the order of 10^{-3}—10^{-5}), calls for a special discussion. The probability of spontaneous emission of a photon in the centimeter band in an electric dipole transition is of the order of 10^{-7} sec^{-1}[70,71], and the probability of nonradiative transitions due to molecule collisions at a pressure on the order of 100 mm Hg is of the order of 10^9 sec^{-1}. It might appear therefore that even when the exciting radiation is completely absorbed not more than 10^{-16} of its energy can be transformed into the third harmonic. Unlike the ammonia maser, in which the frequency ω_0 is excited directly, to generate the third harmonic it is necessary that the lower level have a higher population than the upper level. Therefore amplification at a frequency ω_0 at the expense of stimulated emission cannot take place. The main cause of the high efficiency of conversion lies in the increase in the probability of radiative transition from the excited state into the normal one, owing to the interference phenomena in the ensemble of the molecules. As shown in Sec. 1 of this chapter, using resonant fluorescence as an example, the total probability of scattering is proportional to N^2 if all N molecules are concentrated in a volume smaller than the cube of the wavelength. This phenomenon differs from resonant fluorescence only in that during the course of excitation there is absorbed not one but three photons. Formally, this is equivalent only to replacing k_ρ in (45) by $3k_\rho$, which does not change the deduction that the probability of the elementary act of scattering by an ensemble of molecules is increased and that its reciprocal τ is reduced by a factor N. By N must be meant here the difference in number of molecules in the lower and upper states ΔN, since this difference

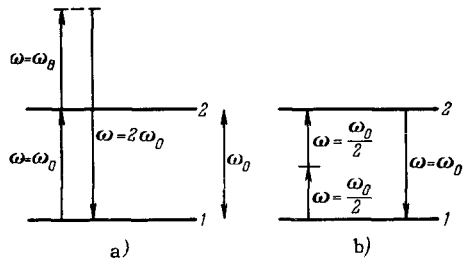

FIG. 22. Possible variants of resonant frequency doubling in a two-level scheme with dipole magnetic transitions.

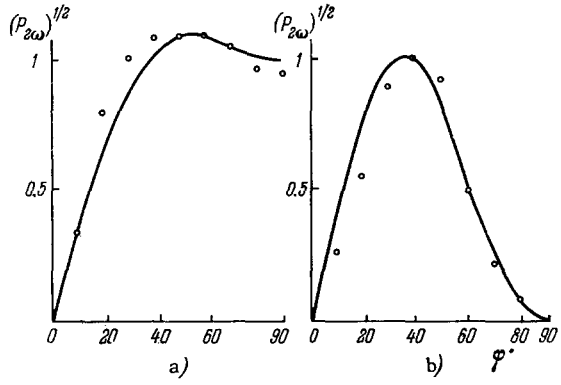

FIG. 23. Dependence of $(P_{2\omega})^{1/2}$ (in arbitrary units) on the angle Φ between $\mathbf{H}$ and $\mathbf{H}_\omega$ ($\mathbf{H}_\omega \perp \mathbf{H}$, $\mathbf{H}_{2\omega} \perp \mathbf{H}_\omega$) for $H = \omega/\gamma$ (Fig. 22a) and $H = 2\omega/\gamma$ (Fig. 22b). Continuous curves – theoretically predicted relations, circles – experimental results.

determines the process of third-harmonic generation. In addition, additional reduction in τ is connected with an increase in the density of the states of the radiation field in the resonator, compared with the density of these states in free space. An analysis shows[70] that this leads to a reduction of τ by a factor $Q\lambda^3/8\pi^2 V$, where V and Q are the volume and quality factors of the loaded cavity, and λ is the wavelength of the scattered radiation. Thus,

$$\tau_{ef} = \tau \frac{8\pi^2 V}{\Delta N Q \lambda^3}. \qquad (52)$$

This expression coincides with the result of a rigorous theoretical analysis [see, for example,[72] formula (7)]. For the experiment described, $\Delta N \approx 10^{16}$, $Q \approx 10^3$, $\lambda_3 \approx V$, and consequently $\tau_{ef} \approx 10^{-17}\tau$, thus explaining the high efficiency of generation of a third harmonic in the ammonia.

A detailed analysis of the possibilities of excitation of the second harmonic in the centimeter band in two- and three-level systems with magnetic dipole transitions is contained in[72]. For frequency doubling in a two-level system it is necessary that the particles have constant dipole moment and that there be an excess of particles in the lower energy state. The theory of the phenomenon predicts two possibilities for resonant frequency doubling: first, when the exciting field has a frequency ω equal to the transition frequency ω_0, and second when $\omega = \omega_0/2$ (Fig. 22). These cases differ appreciably in the dependence of the second-harmonic power $P_{2\omega}$ on the angle Φ between the constant field H, which sets the transition frequency ω_0, and the orientation of the field H_ω (all three vectors H, H_ω, and $H_{2\omega}$ lie in one plane), which excites the generation of the third harmonic. If $\omega = \omega_0$, then $P_{2\omega} \sim [\sin\Phi(1 + \cos^2\Phi)]^2$, and if $\omega = \omega_0/2$ we have $P_{2\omega} \sim [\sin\Phi \cos^2\Phi]^2$. The maximum conversion efficiencies at $\Phi = \Phi_{optim}$ will be of the same order.

Frequency doubling was investigated experimentally for the system of sublevels of the ground state of the free radical diphenyl picryl hydrazyl (DPPH). Polycrystalline samples of DPPH were placed in a rectangular cavity with two resonant frequencies 9500 and 1900 Mcs, placed in a constant magnetic field H, which set the transition frequency ω_0 ($\omega_0 = \gamma H$, where γ—gyromagnetic ratio of DPPH). In accordance with the theoretical predictions, two resonant frequency-doubling modes were observed: when $H = \omega/\gamma$ (case a on Fig. 22), and for $H = 2\omega/\gamma$ (case b on Fig. 22). An investigation of the angular dependence $P_{2\omega}(\Phi)$ (the magnitude of the angle Φ was varied by rotating the magnet that set the field H in the plane of the fields H_ω and $H_{2\omega}$) has shown (Fig. 23) that the experimental dependences are in good agreement with the theoretical ones, and the optimal efficiencies for conversion also turned out to be of the same order, in accord with the theory.

The different angular dependence $P_{2\omega}(\Phi)$ for $\omega = \omega_0$ and $\omega = \omega_0/2$ can be attributed to the difference in the resonant sequence of absorption and emission of photons in these two cases. Thus if $\omega = \omega_0/2$ the resonant contributions to the composite matrix element determining the probability of excitation of the second harmonic give the following two sequences of elementary acts: a) a photon with frequency ω is absorbed—the molecule goes over from the state 1 into 2, a second photon is absorbed with frequency ω—the molecule remains in state 2, a photon with frequency ω_0 is emitted—the molecule returns to state 1; b) a photon with frequency ω is absorbed—the molecule goes over into state 2, a photon with frequency ω_0 is emitted—the molecule returns to state 1. According to (30), the composite matrix element of such a three-photon process is proportional to

$$(\mu\mathbf{H}_\omega)_{12}(\mu\mathbf{H}_{2\omega})_{21}[(\mu\mathbf{H}_\omega)_{11} - (\mu\mathbf{H}_\omega)_{22}] \sim \sin\Phi\cos^2\Phi,$$

where μ—operator of magnetic dipole moment. A similar analysis for the case $\omega \approx \omega_0$, when the resonant contribution is made by processes that start with absorption of a photon with frequency ω and transition of the molecule into state 2, while the remaining sequences of emission (absorption) and transitions of the molecule can be arbitrary, lead to a relation $(P_{2\omega})^{1/2} \sim \sin\Phi(1 + \cos^2\Phi)$.

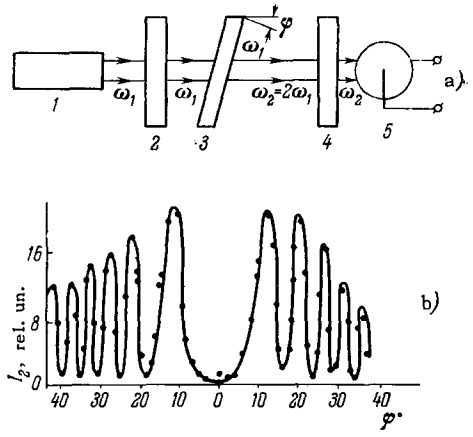

FIG. 24. a) Simplest scheme for second harmonic generation. 1 – Ruby laser; 2 – filter for ruby-laser wavelength, 3 – quartz crystal slab; 4 – filter for second-harmonic wavelength; 5 – photoelectric receiver. b) Dependence of the second-harmonic intensity on the angle between the direction of the laser beam and the normal to the surface of the quartz slab.

Theoretical[72-74] and experimental[72,75,76] investigations of three-level systems for the generation of harmonics and for parametric frequency conversion have shown that such systems, in the presence of double resonance (two of the frequencies are equal to two transition frequencies in the three-level system) are more effective than two-level ones. Exact calculation[72] gives an increase in the conversion efficiency by a factor $(\tau\omega)^2$, where τ—relaxation time constant, which is inversely proportional to the level width. A feature of such systems is that saturation is attained at relatively lower excitation powers, compared with two-level systems, so that a limit is imposed on the maximum power of output radiation in such a system. To prevent saturation, it is necessary to choose systems with minimal relaxation time constants τ. At the present time, in view of the inadequate investigation of the possibilities of three-level systems, it is difficult to arrive at any conclusions relative to the possibility of practical use of these systems[72].

2. Generation of second harmonic in the optical band. Second harmonic generation (SHG) in the optical band was first observed by passing through a quartz crystal a focused beam from a ruby laser, with average power on the order of 10 kW (Fig. 24a)[77]. Radiation with wavelength λ = 3500 Å and power on the order of 10^{-3} W was observed in the transmitted light. These experiments were subsequently repeated with many other crystals (potassium dihydrophosphate (PDP), ammonium dihydrophosphate (ADP), barium titanate, cadmium sulfide, etc.[78-81]), and the mechanism of harmonic generation was thoroughly investigated theoretically[82-92]. Almost all the crystals used for SHG are transparent at both the fundamental and second-harmonic frequency. SHG in such crystals corresponds to a nonresonant three-photon process, in which two photons of the incident radiation are absorbed and one photon with double energy is emitted; the scattering system (crystal) remains in its ground state. According to Sec. 2 of Chapter I, such a three-photon process can occur, in the dipole electric approximation, only in crystals without a symmetry center.

A feature of SHG in crystals is that simultaneous fulfillment of the energy and momentum conservation laws of the photons

$$2\hbar\omega_1 = \hbar\omega_2, \quad 2\hbar\mathbf{k}_1 = \hbar\mathbf{k}_2 \tag{53}$$

(ω_1 and ω_2 are the frequencies of the incident and generated photons, and $\mathbf{k}_1$ and $\mathbf{k}_2$ their wave vectors) is impossible in the general case, owing to the presence of dispersion. Therefore, effective frequency conversion in the second harmonic is possible only in a limited number of crystals (PDP or ADP), in which the photon energy and momentum conservation laws are satisfied for certain directions of propagation of the exciting radiation. It will be shown below that these directions are characterized by definite phase relations between the waves of the fundamental and doubled frequencies. In addition, we shall consider the effect of the crystal intrinsic absorption on the SHG.

a) Second harmonic generation and crystal symmetry. The role of the crystal symmetry in SHG is simplest to illustrate in the semiclassical theory of this phenomenon. In this theory, radiation of the second harmonic is connected with the nonlinearity of the polarization P (dipole moment per unit time), induced by the incident light wave. The dependence of the polarization P on the electric field of the incident light wave can be written in the form*

$$P = \chi E + dE^2 + bE^3 + \ldots \tag{54}$$

Here χ—usual linear optical polarizability, and d and b—coefficients characterizing the nonlinearity of the optical polarizability. The SHG process is described by the second term of (54), which contains a term proportional to cos $2\omega t$ in the case of a sinusoidal field $E = E_1 \sin \omega t$. A discussion of the absolute values of the coefficients d for real crystals will be given later; we note here only that this coefficient is so small that only laser light sources can provide a field intensity E_1 necessary to obtain a detectable second-harmonic intensity.

In isotropic media (such as glass) and in crystals having a symmetry center (such as calcite), for which SHG is forbidden in the electric dipole approximation, the coefficient d is so small that even when lasers are used no SHG is observed. Nonetheless, SHG can be obtained in such a crystal by applying to it a constant electric field. The possibility of this is clear from an

*This expression reflects only the schematic dependence of P on E, which in fact has a tensor nature (see below).

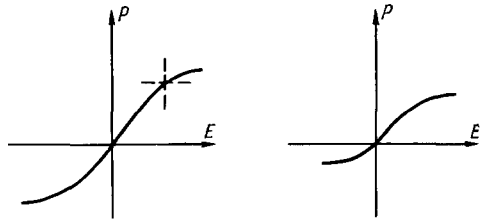

FIG. 25. Schematic representation of the dependence of the polarization P on the amplitude of the electric field E of the light wave: a) For crystals with an inversion center (calcite); b) for crystals without an inversion center (quartz).

examination of Fig. 25, which shows schematically the dependence of P on E for crystals with (a) and without (b) symmetry centers. The asymmetrical (relative to the origin) plot of P vs. E, which is essential for SHG, can be obtained by shifting the origin through application of a constant external field (dashed lines on Fig. 25a). This effect is observed in calcite when a constant electric field with intensity up to 250 kV/cm is applied to a crystal perpendicular to the direction of propagation of the light of a ruby laser[93].

The absence of a symmetry center in a crystal, suitable for an effective SHG process, is a necessary condition for the crystal to have piezoelectric properties. This explains why piezoelectrics are primarily used for SHG. In the general case, the dependence of the quadratic optical polarizability has a tensor character:

$$P_i^{(2)} = \sum_{j,k} d_{ijk} E_j E_k , \tag{55}$$

and the crystal properties that are essential for SHG are determined generally speaking, by the 18 independent elements of the tensor d_{ijk}. Inasmuch as the order of writing down E_j and E_k has no physical meaning (in photon language it corresponds to the order with which the photons from the incident radiation are absorbed), the coefficients d_{ijk} can be written in the abbreviated form used for piezoelectric crystals: the symbols j and k are replaced by a single symbol m, which runs through values from 1 to 6 ($d_{i11} = d_{i1}$, $d_{i22} = d_{i2}$, $d_{i33} = d_{i3}$, $d_{i23} = d_{i4}$, $d_{i31} = d_{i5}$, $d_{i12} = d_{i6}$). The establishment of the form of the tensor P_i^2 is facilitated by the fact, shown in[77,78] that in piezoelectric crystals it should coincide with the form of the piezoelectric tensor. In particular, for ADP and PDP crystals

$$\mathbf{P}_i^{(2)} = \begin{bmatrix} 0 & 0 & 0 & d_{14} & 0 & 0 \\ 0 & 0 & 0 & 0 & d_{14} & 0 \\ 0 & 0 & 0 & 0 & 0 & d_{36} \end{bmatrix} \begin{bmatrix} E_x^2 \\ E_y^2 \\ E_z^2 \\ 2E_yE_z \\ 2E_xE_z \\ 2E_xE_y \end{bmatrix}, \tag{56}$$

and for quartz

$$\mathbf{P}_i^{(2)} = \begin{bmatrix} d_{11} & -d_{11} & 0 & d_{14} & 0 & 0 \\ 0 & 0 & 0 & 0 & -d_{14} & -d_{11} \\ 0 & 0 & 0 & 0 & 0 & 0 \end{bmatrix} \begin{bmatrix} E_x^2 \\ E_y^2 \\ E_z^2 \\ 2E_yE_z \\ 2E_xE_z \\ 2E_xE_y \end{bmatrix}. \tag{57}$$

As to the values of the coefficients of the second-order polarization tensor, they do not coincide with the values of the coefficients of the piezoelectric tensor, inasmuch as SHG in crystals has an electron mechanism, while the piezoeffect is ionic[78]. It was shown, first from thermodynamic consideration[94] and then from the general properties of symmetry of the second-order polarization tensor for a medium in which the dispersion and absorption in the region of the converted frequency and its second harmonic are zero[78], that the tensor elements should be subject to additional limitations that are tantamount to requiring that $d_{ijk} = d_{jik}$. This condition reduces the number of independent elements d_{ijk}. In particular, it leads to $d_{14} = d_{36}$ in potassium and ammonium dihydrophosphate crystals, and $d_{14} = d_{25} = d_{36}$ in quartz. However, since $d_{36} = 0$ by virtue of the symmetry of quartz, we get also $d_{14} = d_{25} = 0$.

A theoretical discussion of the question of the correctness of the additional condition of symmetry for real crystals[78,82,84,94] has shown that the answer can be provided only by quantitative measurements of the second-order polarization tensor elements d. Figure 26 shows the scheme of an experiment aimed at checking the additional symmetry in quartz[95]. A slab 2 mm thick was cut from a quartz crystal in such a way that the Y axis lies in its plane, and the X (twofold symmetry axis) and Z (optical axis of three-fold symmetry) axes make an angle of 45° with its plane. An unfocused polarized laser beam is incident normally on the slab. Under these conditions, (57) yields

$$\mathbf{P}_i^{(2)} = d_{11}E_x^2\mathbf{i} - 2d_{14}E_xE_z\mathbf{j}. \tag{58}$$

Analyzing the transmitted light with the aid of a polarization element, we can separate and compare the contributions made to the second harmonic by d_{11} and d_{14}. Such a comparison has shown that $d_{14} \ll d_{11}$ when either a ruby or a neodymium laser is used. Consequently, additional symmetry is satisfied in the quartz and the second-order polarization tensor reduces to a single element d_{11}.

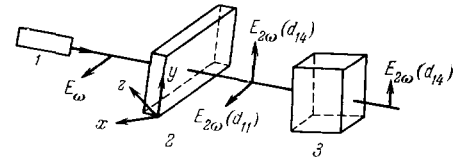

FIG. 26. Diagram of experimental setup for the investigation of the influence of quartz symmetry on SHG. 1 – Ruby laser; 2 – quartz plate; 3 – Glan-Thomson prism.

Table III. Relative values of the elements of the second-order polarizability tensor d and the coherence length l_k for some crystals (d_{36} for PDP is taken equal to unity).

Crystal	Laser	d	(exper.) μ	(calc.) μ
KH_2PO_4	Ruby	$d_{36}=1.00$	18.5	18.8
		$d_{14}=0.95\pm0.06$	7.3	7.2
KD_2PO_4	»	$d_{36}=0.75\pm0.02$	20.6	—
		$d_{14}=0.76\pm0.04$	7.7	—
$NH_4H_2PO_4$	»	$d_{36}=0.93\pm0.06$	17.7	18.2
		$d_{14}=0.89\pm0.04$	6.7	6.4
KH_2PO_4	Neodymium	$d_{36}=1.00$	22.0	22.0
		$d_{14}=1.01\pm0.05$	14.6	15.0
KD_2PO_4	»	$d_{36}=0.92\pm0.04$	21.2	—
		$d_{14}=0.91\pm0.03$	15.8	—
$NH_4H_2PO_4$	»	$d_{36}=0.99\pm0.06$	21.0	20.6
		$d_{14}=0.98\pm0.05$	13.2	13.0
CdS	»	$d_{15}=35\pm2$	1.8	1.9
		$d_{31}=32\pm2$	1.7	1.6
		$d_{33}=63\pm4$	1.8	1.7
$BaTiO_3$	»	$d_{15}=35\pm3$	3.1	—
		$d_{31}=37\pm3$	5.8	—
		$d_{33}=14\pm1$	4.1	—

Subsequently the relative values of the non-zero components of the polarizability second-order tensor were obtained for the crystals of potassium dihydrophosphate (PDP) (KH_2PO_4), ammonium dihydrophosphate (ADP) ($N_4H_2PO_4$), CdS, and $BaTiO_3$[81]. The results of these experiments are listed in Table III, from which it is seen that the equalities dictated by the requirement of additional symmetry, namely $d_{14} = d_{25} = d_{36}$ for ADP and PDP crystals and also deuterated crystals, and $d_{15} = d_{31}$ for the other two crystals, are satisfied within the accuracy of the measurements.

The values of the components d_{33} are different in the crystals CdS and $BaTiO_3$, with the value in CdS exceeding the value of d_{36} for PDP by a factor 63. This means that the SHG efficiency in CdS crystals should be approximately 4000 times larger than in PDP. However, as will be shown below, interference phenomena in PDP and ADP crystals lead to an opposite ratio.

The difficulty in determining the absolute values of the elements of the polarizability tensor when using solid-state lasers is connected with the multi-mode nature of their radiation, which has not yet been adequately studied. A value $d_{36} = (3 \pm 1) \times 10^{-9}$ cgs units was obtained in[96] for PDP, using a continuous-operation He-Ne laser. Using this value one can obtain the absolute values of the remaining elements d listed in Table III.

b) Interference phenomena in SHG. An obstacle to the increase in the efficiency of SHG by simply increasing the light-path length in a transparent crystal is the dispersion of the radiation. To explain the role of the latter, let us examine a plane wave of fundamental radiation, propagating through a crystal slab of thickness l and of infinite length and width (Fig. 27a)[78]. Let us find an expression for the intensity of radiation of the second harmonic on the real surface of the plate, produced by the component of quadratic polarization. Disregarding the tensor connection between P and E, which is inessential for this analysis, we make use of relation (54). If the electric field of the primary light wave is $E = E_1 \cos(\omega_1 t - \mathbf{k}_1 \cdot \mathbf{r})$, then the component of quadratic polarization is

$$P^{(2)}(2\omega_1) = \frac{d}{2} E_1^2 \cos(2\omega_1 t - 2\mathbf{k}_1 \mathbf{r}). \qquad (59)$$

Consequently, the spatial distribution of the polarization at each instant of time is given by $\cos(2\mathbf{k}_1 \cdot \mathbf{r})$, whereas the spatial distribution of the second harmonic of radiation inside the crystal is given by $\cos(\mathbf{k}_2 \cdot \mathbf{r})$. When $2\mathbf{k}_1 \neq \mathbf{k}_2$, the phase difference between the second harmonic of the radiation and the harmonic of the quadratic polarization varies contin-

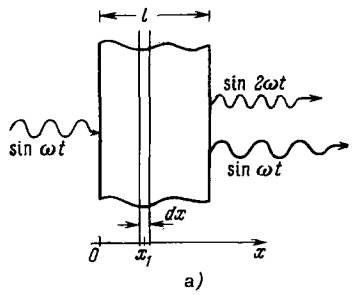

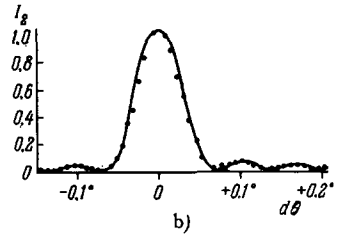

FIG. 27. a) Schematic representation of the generation of a second harmonic in a plane crystal slab with infinite transverse dimensions. b) Dependence of the intensity of the second harmonic in PDP on the angle $d\theta$ between the synchronism direction and the He-Ne laser beam for $\chi = 1.23$ cm.

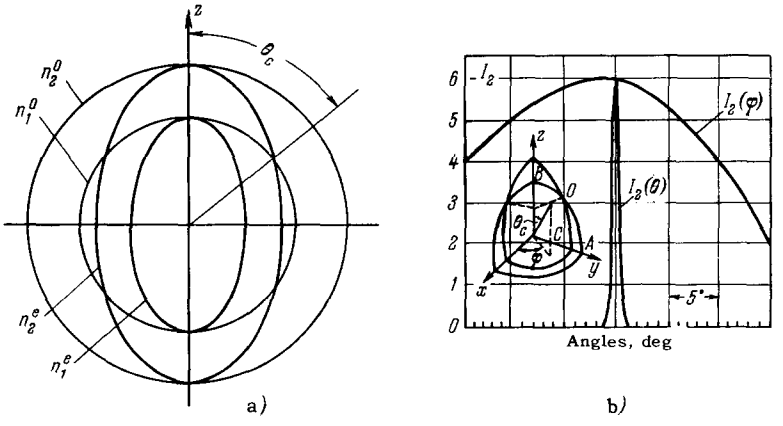

FIG. 28. a) Refractive-index surfaces of PDP crystal. The indices 1 and 2 pertain to the fundamental and second harmonic of the ruby laser, respectively. The indices o and e pertain to the ordinary and extraordinary rays respectively. b) Dependence of the intensity of the second harmonic in PDP on the direction. The maximum intensity is observed at $\theta = \theta_c = 52° \pm 2°$, $\varphi = 45°$. The divergence angle of the laser beam is $\pm 1/4°$. AOB – arc on the refractive-index surface of the ordinary laser ray, COD – for the extraordinary second-harmonic ray.

uously. Consequently, the phase difference between the radiation harmonics produced by the quadratic polarization in different regions of the crystal also varies continuously.

On the rear surface of the crystal slab, that is, at $x = l$, the radiation produced by the quadratic polarization of a layer dx will be

$$dE_2 \sim dx \cos[2\omega_1 t_1 - 2k_1 x_1 + \omega_2 (t - t_1) - k_2 (x - x_1)]_{x=l}$$
$$= dx \cos[\omega_2 t - 2k_1 x_1 - k_2 (l - x_1)]. \quad (60)$$

Consequently, the total field of the wave with frequency $2\omega_1 = \omega_2$ is

$$\int_0^l dE_2 \sim \frac{\sin l(2k_1 - k_2)/2}{2k_1 - k_2} \cos(2\omega_1 t + lk_1 + lk_2/2),$$

and the intensity of the second harmonic of radiation is

$$I_2 \sim \frac{\sin^2 l(2k_1 - k_2)/2}{(2k_1 - k_2)^2} \sim \frac{\sin^2 (n_1 - n_2)\, l\omega/c}{(n_1 - n_2)^2}. \quad (61)$$

In the absence of dispersion ($n_1 = n_2$), the intensity of the second harmonic increases in proportion to the square of the thickness l of the slab. On the other hand, if $n_1 \neq n_2$ then $I_2 = I_2(l)$ has an oscillating character; the oscillation period is

$$l_k = \frac{\lambda}{2(n_1 - n_2)}, \quad (62)$$

where λ—wavelength of radiation of the fundamental frequency in free space, customarily called the coherence length[86]. The maximum intensity of the second-harmonic radiation is obtained when $l = (2q + 1) l_k/2$, where q is an integer. The coherence lengths in typical crystals used for SHG are of the order of 10^{-3}—10^{-4} cm (see Table II).

Expression (61) coincides with relation (49) for the intensity of the elementary act of scattering by N identical centers located at equal distances from one another on a length l; the latter relation was obtained from quantum considerations. As already mentioned, the interference phenomena are based on the interference of the probabilities of the elementary act of scattering by an ensemble of scattering centers, as a result of which the intensity obtained for the scattering by N centers is not equal to the sum of the intensities of scattering by each of the N centers.

The maxima and minima of intensity of the second harmonic as functions of the length of the crystal were first observed experimentally for SHG in quartz[97]. The change of the length l in a scheme analogous to that shown in Fig. 24a was realized by rotation of the crystal slab about an axis perpendicular to the direction of light propagation. The dependence observed in this case of the intensity of the second harmonic on the angle of incidence of the beam is shown in Fig. 24b. The angular distances between the maxima agree with the quantities given by expression (61). In some uniaxial crystals, the condition $n_1 = n_2$ (the synchronism condition) can be satisfied for waves with fundamental and second-harmonic frequencies of different polarizations, which makes it possible to increase greatly the SHG efficiency. Figure 28a shows schematically the dependence of the refractive indices n^o and n^e of the ordinary and extraordinary rays in a PDP crystal on the direction for the fundamental frequency of a ruby laser (n_1^o and n_1^e) and for the second-harmonic frequency (n_2^o and n_2^e). The phase velocity of the ordinary ray is the same for all directions, while that of the extraordinary ray depends on the direction of its propagation and coincides with the phase velocity of the ordinary ray of the same frequency only for propagation along the optical axis (the z axis on Fig. 28a). At the same time, there are propagation directions, making an angle θ_c with the optical axis, for which the refractive index of the ordinary ray with fundamental frequency n_1^o is equal to the refractive index of the extraordinary ray with double the frequency n_2^e. This "synchronism" angle in the PDP crystal is equal to approximately 50° for ruby-laser radiation. An increase in the intensity of the second harmonic for radiation propagating in the direction of the synchronism angle, amounting to several orders of magnitude, was first demonstrated in[97,98]. The dependence of the SHG efficiency on the angle θ is quite strong, and

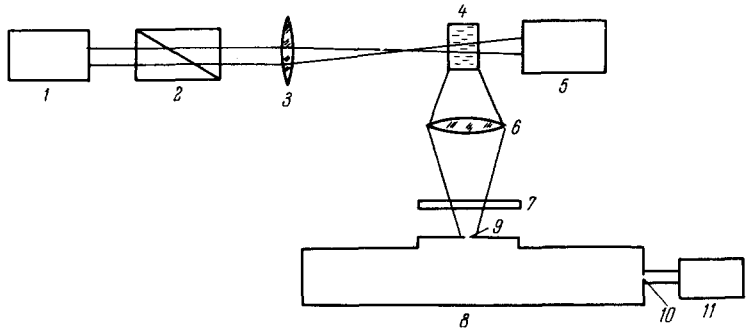

FIG. 29. Experimental set-up for the measurement of absolute values of the Raman scattering cross section. 1 – Ruby laser; 2 – polarizer, 3 – con ensing lens; 4 – cuvette with investigated liquid; 5 – exciting-radiation detector; 6 – gathering lens; 7 – filter blocking the laser radiation; 8 – spectrograph; 9 – spectrograph entrance slit; 10 – spectrograph exit slit; 11 – scattered radiation detector.

when the angle between the ray and the synchronism direction increases by a fraction of a degree, the intensity of the second harmonic is reduced to one-half (Fig. 28b). The SHG efficiency exhibits also a weak dependence on the azimuthal angle φ (angle between the direction of radiation propagation and the xOz plane). This dependence is connected with the symmetry properties of the quadratic-polarization tensor in such a way that the tensor component which determines the SHG turns out to be proportional to $E_x E_y \sim \sin\varphi\cos\varphi$.

A quantitative check on the angular dependences of the SHG efficiency was made in[96], using an He-Ne laser ($\lambda = 1.1526\,\mu$). The experimental points (Fig. 27b) are in good agreement with the theoretical curve. The absolute value of the nonlinear polarizability of the PDP for one-mode gas laser operation was found to be $d_{36} = (3 \pm 1) \times 10^{-9}$ cgs units. Owing to the low power of the gas laser (1.5×10^{-3} W), the conversion efficiency was low (the second-harmonic power was of the order of 8×10^{-14} W). It is interesting to note from the theoretical point of view that in the direction of exact synchronism the entire energy of the fundamental harmonic can be converted into the second harmonic[79,83].

c) Effect of crystal intrinsic absorption on SHG efficiency. A classical analysis using a nonlinear harmonic oscillator as a model of electron motion in the crystal predicts an abrupt increase in the intensity of the second harmonic as its frequency approaches the edge of the intrinsic absorption band of the crystal[78,82]. On the other hand, a quantum-mechanical analysis with account of the crystal absorption band structure shows that there should be no sharp increase in the second-harmonic power in this case[84]. The case when the frequency of the second harmonic falls in the crystal absorption band was not considered theoretically; it was assumed that the large absorption will not make it possible to obtain in this case a noticeable radiation at the doubled frequency.

For an experimental investigation of the influence of the intrinsic absorption of the crystal on the SHG efficiency, the temperature shift of the edge of the intrinsic absorption of the CdS crystal was used[81]. At room temperature, this edge lies near 2.48 eV and exceeds by 0.14 eV the energy of the double-frequency quantum radiated by a neodymium laser, $\hbar\omega_2$. When the temperature is increased to approximately 235°C, the edge of the absorption edge is displaced until it coincides with $\hbar\omega_2$. Measurements of the second-harmonic intensity as a function of the temperature in the range 25–300°C have shown that the SHG efficiency remains practically constant and no increase was observed for it near 235°C.

An investigation of SHG under conditions when the second harmonic falls in the band of the intrinsic absorption of the crystal was made using a ruby laser in CdS and $BaTiO_3$, and also in GaAs with a neodymium laser[81]. It was shown that absorption does not hinder the SHG, and that in the case of CdS and $BaTiO_3$ its efficiency is comparable with the efficiency of conversion of the ruby laser beam propagating perpendicular to the {110} plane in a PDP crystal. The values of the coefficients of the tensor d obtained in the paper are listed in Table III.

The possibility of relatively effective generation of a harmonic in a crystal, even if its frequency falls in the intrinsic absorption band, can be understood qualitatively by recognizing that the coherence length in these crystals is of the order of 10^{-4} cm. Therefore only the last layer of the crystal participates effectively in the generation of the second harmonic, and in this layer the absorption of the second harmonic remains small.

3. Some phenomena in Raman scattering (RS) of laser radiation. *a) Experimental determination of Raman scattering cross sections.* Owing to their narrow emission spectrum and the high emission intensity and directivity, lasers are of great interest for the excitation of Raman spectra. A special analysis has shown that lasers have undisputed advantages over such traditional radiation sources as a mercury lamp for the excitation of the spectra of crystalline samples of small size and of gases, and also in many other cases[122-125]. The use of a ruby laser has made it possible to determine for the first time the absolute values of the RS cross section of several lines of benzene, nitrobenzene, and toluene[126]. A diagram of the installation used for this purpose is shown in Fig. 29. The radiation of the ruby laser could be polarized

Table IV. Measured values of the Raman scattering cross section

Raman scattering line, cm^{-1}	Total width of Raman scattering line at 0.5 maximum value, cm^{-1}	Polarization ratio $\sigma_{\parallel}/\sigma_{\perp}$	$\sigma_{\perp}$, cm^{-2}
Nitrobenzene 1345	11 ± 0.4	0.22	2.3
Benzene 991.6 . .	3.1	0.06	3.9
Benzene 1179 . .	15.7	0.7	0.13
Toluene 1102 . .	2.7	0.06	1.1
Toluene 1212 . .	3.2	0.12	0.24

either parallel or perpendicular to the plane containing the exciting and scattered rays (scattering plane) by changing the position of the polarizer. The receivers were calibrated photomultipliers. Table IV lists the measured maximum values of the RS cross sections per unit wavelength interval of the RS line, per unit volume of the scattering material, and per unit solid angle in which the scattering takes place. The RS cross section depends on the position of the plane of polarization of the incident radiation relative to the observation direction. In the third column of Table IV is given the ratio of the cross sections of RS in the case of plane polarization parallel and perpendicular to the observation direction ($\sigma_{\parallel}$ and $\sigma_{\perp}$, respectively).

b) Stimulated Raman scattering. The use of lasers has made it possible to observe some new Raman scattering phenomena of considerable fundamental interest. These include stimulated RS, first observed in the investigation of a Q-switched ruby laser, the modulator used being a Kerr cell with nitrobenzene, placed in a cavity[127]. It was found that under these conditions there is observed, besides the stimulated emission with wavelength 6940 Å, also additional intense radiation with $\lambda = 7670$ Å. The latter phenomenon was observed with the aid of a cuvette with nitrobenzene inside the interferometer of a Q-switched laser with a PDP crystal. It was established that the additional emission displays several characteristic properties of stimulated emission: a sharp threshold of occurrence both when the ruby laser power is varied and when the length of the cuvette with the liquid is varied, a sharp directivity (divergence angle on the order of 1 mrad), and a decrease in radiation line width with increasing laser beam power. In subsequent investigations the additional emission was obtained in many organic and inorganic liquids[128-130], and also in crystals[133,134] and gases[135] that are active to RS. It was found that the shifts of the additional-emission line frequencies corresponded to the tabulated shifts of the most intense RS lines of the investigated substance.

All these factors, and also the absence of resonant absorption of the ruby-laser emission in the investigated substances (for most of the substances the absorption coefficient was of the order of 10^{-3} cm^{-1}), indicates that the additional emission is stimulated Raman scattering.

An examination of the mechanism of stimulated RS on the basis of quantum and semiclassical theory of multiphoton processes is given in[136-145]. In quantum theory, Raman scattering is regarded as a two-photon scattering process, consisting in the absorption of a single photon of the exciting radiation $\hbar\omega_0$, and emission of a photon $\hbar\omega_{-1}$. The energy difference $\hbar(\omega_0 - \omega_{-1}) = \hbar\omega_i$ is compensated by the transition of the scattering medium to an excited state. The probability of such a process per unit time, equal to the rate of emission of the scattered photons dN_{-1}/dt, is determined by formula (29) and is of the form

$$\frac{dN_{-1}}{dt} = \frac{2\pi}{\hbar} |K_{mn}^{(2)}|^2 \rho_n \Delta N. \qquad (63)$$

Here ΔN—difference in the populations of the initial (m) and final (n) states of the scattering system, $\rho_n = 2/\pi\hbar\Delta\omega_r$—density of the final states ($\Delta\omega_r$—RS linewidth), and $K_{mn}^{(2)}$—composite matrix element of second order, defined by (30). If in the initial state, at a definite laser mode, there are N_0 photons with frequency ω_0, and in a certain scattered-radiation mode there are N_{-1} photons with frequency ω_{-1}, then $|K_{mn}^{(2)}|^2 \sim N_0(1 + N_{-1})$. When $N_{-1} = 0$ (absence of photons in the scattered-radiation mode in question), $dN_{-1}/dt \sim N_0$ and formula (63) describes the process of ordinary ("spontaneous") RS. If $N_{-1} \neq 0$, then the probability that the photons will enter into a mode with frequency ω_{-1} consists of the probability of spontaneous emission and the probability of stimulated emission. The latter is equal to the number of photons in the mode in question, multiplied by the probability of spontaneous emission. Like stimulated fluorescence in lasers, stimulated emission in RS can lead to an intensification of the scattered radiation, and then also to generation if this intensification exceeds the losses in the resonator tuned to the frequency ω_{-1}.

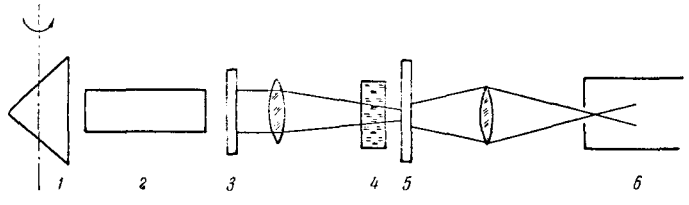

FIG. 30. Experimental set-up for the observation of Raman scattering of laser radiation. 1 – 3 – Rotating prism, ruby rod with illuminator, and semitransparent reflecting mirror of Q-switched laser; 4 – cell with substance active to Raman scattering; 5 – diffuse scatterers; 6 – spectrograph.

The essential difference between stimulated RS and stimulated emission in lasers lies in the fact that in RS there is no need for inverting the populations of the states of the scattering system. Moreover, for stimulated RS at a frequency ω_{-1} it is necessary to have $\Delta N = N_m - N_n > 0$, and the amplification coefficient ($\alpha_{-1} \sim dN_{-1}/dt$) is proportional to $\Delta N = N_m - N_n$. The condition $N_m > N_n$ is satisfied under thermodynamic equilibrium and is not violated in practice during the RS process. The latter is connected with the fact that even in the more intense giant pulsed lasers the photon flux does not exceed 3×10^{18} per cm^2, so that, for example in liquids, less than one out of 10^4 molecules goes over from the initial state.

Stimulated emission of RS is obtained under dynamic equilibrium in systems with very small RS cross sections compared with the cross section for resonance fluorescence, inasmuch as the RS is a nonresonant process. It is impossible at present to calculate the RS cross sections theoretically. In[136,137] there was developed a phenomenological theory of stimulated RS, based on the RS cross section determined experimentally (see Table IV). The threshold intensity of the incident radiation necessary to attain the generation mode can be estimated by starting from the relation $\alpha_{-1} \cdot 2l > \alpha_L$, where α_{-1}—amplification coefficient at frequency ω_{-1} and α_L—loss coefficient in the ω_{-1} mode for a complete cyclic passage of the photon through the resonator. This relation means that amplification at two passages of the cuvette with the investigated substance of length l should exceed the total losses α_L. The maximum coefficient α_{-1} is connected with the maximum RS cross section $\sigma_\perp$ in the following fashion[137]:

$$\alpha_{-1} = \frac{I_0 \sigma_1 \lambda_{-1}^4}{n_{-1} c}, \qquad (64)$$

where I_0—intensity of the incident radiation, in photons per square centimeter and per second, λ_{-1}—wavelength of RS emission in centimeters, c—velocity of light, and n_{-1}—refractive index of the investigated substance at wavelength λ_{-1}.

An estimate of the required intensity for nitrobenzene ($\sigma_1 = 2.3$ cm^{-2}), at a loss coefficient $\alpha_L = 0.5$ and a length $l = 5$ cm, yields $I_0 \geq 10$ MW/cm^2, which agrees with the experimental data[128,137]. A theoretical estimate of the line narrowing that results (for a 1% conversion of energy into the CR line) yields[137] a reduction in line width to a value of 0.14 of its initial value, 11 cm^{-1}, that is, to ~ 1.5 cm^{-1}, which also agrees with the experimental data. The maximum conversion efficiency, about 30%, was obtained at the present time in nitrobenzene.

The totality of the results obtained to date on this phenomenon leaves no doubt that the mechanism of stimulated RS exists, although some details of this process are not yet clear. In particular, it is not clear why it is impossible to obtain a generation mode in many liquids possessing very intense lines of ordinary RS.

c) Stimulation of coherent molecular oscillations in RS of laser radiation. A thorough investigation of stimulated RS has led to a discovery of several phenomena, which could not be interpreted within the framework of either ordinary "spontaneous" or stimulated RS. These include the following:

1. Even in the first experiments on stimulated RS there were observed lines that were shifted relative to the ruby-laser emission frequency not only by amounts equal to the frequency of the molecular oscillations ω_r, but also to the multiple frequencies $2\omega_r$, $3\omega_r$, etc (overtones). Measurements of the positions of the lines in the RS spectra of liquid oxygen, nitrogen, and other substances, with instruments having high resolution, has shown that their appearance cannot be attributed to the anharmonicity of the molecular oscillations. Furthermore, lines of multiple frequencies arise at the same threshold value of the primary-beam power as the line with the fundamental frequency ω_r. On the other hand, when the power of the exciting beam increases above the threshold, the intensities of the multiple lines increase rapidly and reach values that are close to the intensity of the fundamental line of the scattered radiation. On the other hand, in ordinary RS spectra, the selection rule, which forbids the appearance of overtones in first approximation, is sufficiently well satisfied, and the overtone intensity is at least two orders of magnitude lower than the intensity of the fundamental line.

2. In investigations of RS of high-density radiation in substances placed outside the laser resonator, intense coherent emission was observed at frequencies which were not only smaller but also larger than the frequency ω_0 of the laser (anti-Stokes emission). Different anti-Stokes frequencies correspond to different propagation angles relative to the direction of the primary beam, so that in sections perpendicular to the latter there were observed rings of coherent radiation, the color of which changed from yellow to blue. Further thorough study of anti-Stokes emission in liquids[131], crystals[133,134] and gases[135] has shown that it occurs at the same densities of the primary beam as the Stokes emission, but is not observed if the substance that is active in the RS is placed in a laser resonator having plane mirrors. The line shift turned out to be an exact multiple of the frequency of the fundamental oscillation ω_r, the line intensity was close to the intensity of the corresponding Stokes lines, and the narrowing was approximately one order of magnitude larger than the narrowing of the latter. The anti-Stokes radiation was observed even in substances which had none in the ordinary RS spectrum. The latter circumstance indicates that it cannot be connected with the scattering of laser emission by molecules that are in thermodynamic equilibrium in excited vibrational states: v = 1, 2, ...

3. Intense phenomena were observed in RS laser radiation in two liquids—benzene and carbon disulfide—mixed in a ratio 1:1 and placed separately in two cuvettes one after the other along the path of the beam[131]. In the first case, many lines were observed in addition to the lines shifted by the frequencies ω_r of the fundamental oscillations of both liquids and their harmonics (the benzene line was the more intense). They were shifted by frequencies equal to the sum and difference of the vibrational frequencies corresponding to the scattering in each liquid separately. In the second case, no additional lines were observed, although they could be expected as a result of scattering in the second cuvette of harmonics produced in the first. Regardless of the sequence of the liquids, the more intense scattering spectrum lines were produced in carbon disulfide.

Although at present there is no unified theory describing all the new phenomena in Raman scattering, many of them can be understood on the basis of ideas concerning the excitation of coherent molecular oscillations by an intense laser beam[140]. Usually RS is regarded as an incoherent process, in which the phases of the oscillations of the different molecules have a random distribution. It was indicated in[140], however, that stimulated RS which produces radiation at the fundamental Stokes frequency $\omega_0 - \omega_r$, can lead to establishment of definite phase relationships between the oscillations of different molecules. Such coherent oscillations of an ensemble of molecules can modulate the initial radiation (with frequency ω_0) and the radiation of the stimulated RS (with frequency $\omega_0 - \omega_r$), causing the appearance of Stokes and anti-Stokes lines of many orders.

A quantitative theory of these processes is based on examination of the behavior of the molecule, represented as a harmonic oscillator with resonant frequency ω_r, situated in an electric field E containing several harmonic components with definite phase relations. The behavior of the molecule is described by an equation of the type

$$\frac{d^2}{dt^2}x + R\frac{d}{dt}x + \omega_r^2 x = F, \tag{65}$$

in which x—vibrational coordinate and F—driving force. The latter represents, in the semiclassical treatment, the force of interaction between the field and the dipole moment induced in the molecule, $\mu_1 = \alpha E$ (α—polarizability, assumed for simplicity to be isotropic), and which is equal to the negative of the derivative of the dipole polarization energy in the electric field with respect to the vibrational coordinates. In the case of isotropic polarizability this energy is $U = -\alpha E^2/2$, and therefore

$$F = \frac{1}{2}(d\alpha/dx)E^2.$$

If the electric field contains two harmonic components:

$$\mathbf{E} = \mathbf{E}_0 \cos(\omega_0 t - \mathbf{k}_0\mathbf{r}) + E' \cos(\omega' t - \mathbf{k}'\mathbf{r} + \Phi'),$$

where $\mathbf{r}$—radius vector of the molecule position, then the driving force F has a component oscillating at the difference frequency $\omega_0 - \omega'$. If this frequency is in resonance with the natural frequency of the molecule ω_r, then the molecule oscillations build up. A solution of (65) yields at resonance

$$x = \frac{1}{2}\frac{d\alpha}{dx}\frac{(\mathbf{E}_0\mathbf{E}')}{R(\omega_0 - \omega')}\sin[(\omega_0 - \omega')t - (\mathbf{k}_0 - \mathbf{k}')\mathbf{r} - \Phi'].$$

Such a forced oscillation of the molecule leads to the occurrence of a component of the dipole moment

$$\boldsymbol{\mu} = x\frac{d\alpha}{dx}\mathbf{E},$$

whose rate of change of energy with the harmonic of the field $\mathbf{E}'$ at the frequency ω' is

$$P' = -\left\langle\left(\frac{d\boldsymbol{\mu}}{dt}\right)\mathbf{E}'\right\rangle = \frac{1}{8R}\left(\frac{d\alpha}{dx}\right)^2\frac{\omega'}{\omega_0 - \omega'}(\mathbf{E}_0\mathbf{E}')^2 \tag{66}$$

and determines the radiation power emitted or absorbed by the molecule at the frequency ω'. For the Stokes radiation component $\omega' = \omega_0 - \omega_r$, we have $P' > 0$ and the field E' becomes stronger, whereas for the anti-Stokes component $\omega' = \omega_0 + \omega_r$ the field E' weakens.

Amplification of the anti-Stokes component can be obtained if the radiation field is represented by three harmonics in the form

$$\mathbf{E} = \mathbf{E}_0 \cos(\omega_0 t - \mathbf{k}_0\mathbf{r}) + \mathbf{E}_{-1}\cos[(\omega_0 - \omega_r)t - \mathbf{k}_{-1}\mathbf{r} + \Phi_{-1}] + \mathbf{E}_1\cos[(\omega_0 + \omega_r)t - \mathbf{k}_1\mathbf{r} + \Phi_1]. \tag{67}$$

An analysis similar to that given above shows that

$$x = \frac{1}{2R\omega_r}\left(\frac{d\alpha}{dx}\right)\{(\mathbf{E}_0\mathbf{E}_{-1})\sin[\omega_r t - (\mathbf{k}_0 - \mathbf{k}_{-1})\mathbf{r} - \Phi_{-1}] + (\mathbf{E}_0\mathbf{E}_1)\sin[\omega_r t + (\mathbf{k}_0 - \mathbf{k}_1)\mathbf{r} + \Phi_1]\}, \tag{68}$$

$$\left.\begin{aligned} P_{-1} &= \frac{\omega_0 - \omega_r}{8R\omega_r}\left(\frac{d\alpha}{dx}\right)^2\{(\mathbf{E}_0\mathbf{E}_{-1})^2 \\ &\quad + (\mathbf{E}_0\mathbf{E}_1)(\mathbf{E}_0\mathbf{E}_{-1})\cos[(2\mathbf{k}_0 - \mathbf{k}_1 - \mathbf{k}_{-1})\mathbf{r} + \Phi_1 + \Phi_{-1}]\}, \\ P_1 &= \frac{\omega_0 + \omega_r}{8R\omega_r}\left(\frac{d\alpha}{dx}\right)^2\{-(\mathbf{E}_0\mathbf{E}_1)^2 \\ &\quad - (\mathbf{E}_0\mathbf{E}_1)(\mathbf{E}_0\mathbf{E}_{-1})\cos[(2\mathbf{k}_0 - \mathbf{k}_1 - \mathbf{k}_{-1})\mathbf{r} + \Phi_1 + \Phi_{-1}]\}. \end{aligned}\right\} \tag{69}$$

If $E_{-1} > E_1$, then both the Stokes and the anti-Stokes components can become amplified. Continuous amplification of the anti-Stokes component over the entire volume occupied by the ensemble of molecules will occur only if the synchronism condition is satisfied

$$2\mathbf{k}_0 - \mathbf{k}_{-1} - \mathbf{k}_1 = 0 \tag{70}$$

and $\cos(\Phi_1 + \Phi_{-1}) < 0$. Thus, the absence of a random distribution of the phases of the fields E_1 and E_{-1} is necessary in order for amplification of the anti-Stokes component to be possible.

Maximum amplification of the anti-Stokes component

E_1 takes place if $\Phi_1 + \Phi_{-1} = \pi$, that is, in the case when the fields E_1 and E_{-1} force the molecule to oscillate in antiphase: $x \sim (E_{-1} - E_1)$.

In fact, the first to arise is the Stokes component E_{-1}, that is, the condition $E_- > E_1$ is satisfied. In the first approximation, emission of the Stokes component is diffuse and its intensity is proportional to $(\mathbf{E}_0 \cdot \mathbf{E}_{-1})^2$.

The additional angle dependence is connected with the geometry of the cuvette, which determines the difference in the path length of the ray along which amplification can take place. Inasmuch as both the power generated in the Stokes component and the loss are proportional to E_{-1}^2, there is a generation threshold of E_{-1} in any direction, in agreement with experiment.

The anti-Stokes radiation can be amplified only in directions determined by the synchronism condition (70), which is satisfied for some fixed angles to the laser beam direction[140]. The fact that the anti-Stokes radiation cannot build up when the cuvette is situated inside an interferometer with plane mirrors is connected with the fact that the dispersion prevents satisfaction of the synchronism conditions when the waves $\mathbf{E}_0$ and $\mathbf{E}_{-1}$ propagate in the parallel directions of the multiple Stokes and anti-Stokes components of E. A quantitative check on the spatial distribution in calcite[134] and some experiments on the observation of spatial distribution of these components in toluene and benzene[144] give grounds for assuming that the RS mechanism in question actually does occur.*

Relation (69) explains the absence of an additional threshold for the fundamental anti-Stokes component (and, as can be shown, for the Stokes and anti-Stokes components of higher-orders[140]). Indeed, the amplification of the power of the anti-Stokes component is proportional to E_1, whereas the loss is proportional to E_1^2. Therefore, as $E_1 \to 0$ the amplification decreases more slowly than the loss, and starts to exceed the loss at a certain value of E_1.

Using (69), we can show that if at the beginning the field $E_{-1} = E_{-1}(0)$ and $E_1 = 0$, then the growth of the waves over a path l, neglecting their absorption in the medium, will be of the form

$$\left.\begin{aligned} E_{-1}(l) &= E_{-1}(0)\,[1 + \alpha_{-1} l/2], \\ E_1(l) &= E_{-1}(0)\,\alpha_{-1} l/2. \end{aligned}\right\} \qquad (71)$$

E_1 becomes commensurate with E_{-1} when $\alpha_{-1} l/2 \gg 1$. This explains the theoretically considered and experimentally observed generation of Stokes and anti-Stokes components of almost equal intensity.

Finally, the theory considered enables us to explain the mechanism of amplification of RS lines of benzene and the appearance of additional lines when benzene is mixed with carbon disulfide. If the polarizabilities of the two molecules are α_1 and α_2, then the energy of their interaction is approximately equal to the interaction energy $(2\alpha_1\alpha_2/d^3)E^2$ of two dipoles with induced moments (d is the distance between the molecules). This interaction produces an additional force that induces oscillation of the molecules [for example, for molecule 2 this force is $2\alpha_1/d^3\ (d\alpha_2/dx)E^2$]. This additional force is superimposed on the force F, both having a similar dependence on the electric field E, and when $4\alpha_1 > d^3$ the additional force predominates. The greater the polarizability α_1, the greater the additional force. This is precisely the reason for the increased intensity of the RS line of benzene to which strongly polarizable CS_2 molecules are added. It is obvious that since the additional force is proportional to $\alpha_1 (d\alpha_2/dx)$, lines can be produced which are combinations of the vibrational lines of the molecules of both types, as is indeed observed in experiment.

*An anomaly in the spatial distribution of SR was observed in nitrobenzene[132, 145]. Its causes are not sufficiently clear at present.

[1] P. A. M. Dirac, Proc. Roy. Soc. (London), **A114**, 143, 710 (1927).

[2] M. Goeppert-Mayer, Ann. Physik **9**, 273 (1931).

[3] J. Frenkel, Wave Mechanics, Dover, N. Y., 1950.

[4] A. S. Davydov, Kvantovaya mekhanika, Fizmatgiz, 1963.

[5] R. P. Feynman, Quantum Electrodynamics, Benjamin, 1961.

[6] O. V. Konstantinov and V. I. Perel', JETP **39**, 197 (1960), Soviet Phys. JETP **12**, 142 (1961).

[7] L. Mandel and E. Wolf, Phys. Rev. Letts **10**, 276 (1963).

[8] M. Born and E. Wolf, Principles of Optics, London, 1959, p. 501.

[9] L. Mandel, Proc. Phys. Soc. **8**, 1104 (1963).

[10] J. N. Dodd and G. W. Series, Proc. Roy. Soc. **263**, 353 (1961).

[11] O. V. Konstantinov and V. I. Perel', JETP **45**, 279 (1963), Soviet Phys. JETP **18**, 195 (1964).

[12] C. Cohen-Tunnoudji, Thesis (Paris, 1962); Ann. phys. (Paris) **7**, 423 (1962).

[13] V. S. Pugachev, Teoriya sluchaĭnykh funktsiĭ, Fizmatgiz, 1960, p. 127.

[14] W. Heitler, The Quantum Theory of Radiation, Oxford, 1954.

[15] R. Lennuier, J. chim. phys. **46**, 74 (1949); Ann. phys. **2**, 233 (1947).

[16] V. I. Grigor'ev, Vestnik, Moscow State Univ., Math. Ser., No. 6, 71 (1958).

[17] V. Weisskopf, Ann. Physik **9**, 23 (1931).

[18] V. Hughes and L. Grabner, Phys. Rev. **79**, 314, 829 (1950).

[19] Besset, Horowitz, Messiah, and Winter, J. phys. et radium **15**, 251 (1954).

[20] Brossel, Cagnac, and Kastler, J. phys. et radium **15**, 6 (1954).

[21] P. Kusch, Phys. Rev. **93**, 1022 (1954); **101**, 627 (1956).

[22] W. Anderson, Phys. Rev. **104**, 850 (1956).
[23] J. I. Kaplan and S. Meiboom, Phys. Rev. **106**, 499 (1957).
[24] N. Bloembergen and P. Sorokin, Phys. Rev. **110**, 865 (1958).
[25] Sorokin, Gelles and Smith, Phys. Rev. **112**, 1513 (1958).
[26] J. M. Winter, Ann. phys. **4**, 745 (1959).
[27] S. Yatsiv, Phys. Rev. **113**, 1522, 1538 (1959).
[28] A. Kastler, Ann. Arbor Conf. on Optical Pumping, Univ. of Michigan, 1959, p. 71.
[29] G. V. Skrotskiĭ and T. G. Izyumova, UFN **73**, 423 (1961), Soviet Phys. Uspekhi **4**, 177 (1961).
[30] W. Kaiser and C. G. B. Garrett, Phys. Rev. Letts **7**, 229 (1961).
[31] D. A. Kleinman, Phys. Rev. **125**, 87 (1962).
[32] J. D. Abella, Phys. Rev. Letts **9**, 453 (1962).
[33] D. R. Bates and A. Damgaard, Phil. Trans. Roy. Soc. (London) **242**, 101 (1949).
[34] P. M. Stone, Phys. Rev. **127**, 1151 (1962).
[35] J. A. Giordmaine and J. A. Howe, Phys. Rev. Letts **11**, 207 (1963).
[36] Peticolas, Goldsborough and Rieckhoff, Phys. Rev. Letts **10**, 1 (1963).
[37] S. Singh and B. P. Stoicheff, J. Chem. Phys. **38**, 2032 (1963).
[38] Kepler, Caris, Avakian and Abramson, Phys. Rev. Letts **10**, 400 (1963).
[39] Andresen, Welling and Kellington, Phys. Rev. Letts **11**, 361 (1963).
[40] Hopfield, Worlock, and Park, Phys. Rev. Letts **11**, 414 (1963).
[41] K. Teegarden, Phys. Rev. **108**, 660 (1957).
[42] R. S. Knox and N. Inchauspe, Phys. Rev. **116**, 1093 (1959).
[43] J. Ducuing and N. Bloembergen, Phys. Rev. **A133**, 1493 (1964).
[44] L. Mandel, Proc. Third Quantum Electronics Conference, Paris, 1963, ctp. 101.
[45] R. Braunstein, Phys. Rev. **125**, 475 (1962).
[46] R. London, Proc. Phys. Soc. **80**, 952 (1962).
[47] R. Braunstein and N. Ockman, Phys. Rev. **A134**, 499 (1964).
[48] G. D. Mahan and J. J. Hopfield, J. Appl. Phys. **34**, 1531 (1963).
[49] R. E. Makinson, Proc. Phys. Soc. **A64**, 135 (1951).
[50] R. Smith, Phys. Rev. **128**, 2225 (1962).
[51] A. Z. Veksler, Quantum Theory of the Photoeffect and Thermionic Emission from Metals and Semiconductors, Dissertation, Ural State Univ., 1956.
[52] I. Adawi, Phys. Rev. **A134**, 788 (1964).
[53] D. Lichtman and J. Ready, Phys. Rev. Letts **10**, 342 (1963).
[54] S. Geltman, Phys. Letts **4**, 168 (1963).
[55] Sands, Golgrove, and Franken, Ann. Arbor. Conf. on Optical Pumping, 1959, p. 184.
[56] Colgrove, Franken, Lewis, and Sands, Phys. Rev. Letts **3**, 420 (1959).
[57] J. N. Dodd, Proc. Phys. Soc. **77**, 669 (1961); **78**, 65 (1961).
[58] P. Thaddeus and R. Novick, Phys. Rev. **126**, 1774 (1962).
[59] A. Lurio and R. Novick, Phys. Rev. **A134**, 608 (1964).
[60] E. B. Aleksandrov, Konstantinov, Perel', and Khodovoi, JETP **45**, 503 (1963), Soviet Phys. JETP **18**, 346 (1964).
[61] C. J. Favre and E. Geneux, Phys. Letts **8**, 190 (1964).
[62] V. A. Khodovoi, JETP **46**, 331 (1964), Soviet Phys. JETP **19**, 227 (1964).
[63] A. Javan, Phys. Rev. **107**, 1579 (1957).
[64] S. Yatsiv, Phys. Rev. **113**, 1539 (1959).
[65] T. Yajima and K. Shimoda, Advances in Quantum Electronics, Columbia Univ. Press, N. Y.—London, 1961, p. 548.
[66] T. Yajima, J. Phys. Soc. Japan **16**, 1594, 1709 (1961).
[67] Fontana, Pantell, and Smith, Advances in Quantum Electronics, Columbia Univ. Press, N. Y.—London, 1961, p. 612.
[68] Fontana, Pantell, and Smith, Electronics **35**, (19), 42 (1962).
[69] Fontana, Pantell, and Smith, Proc. IRE **50**, 469 (1962).
[70] N. Bloembergen and R. V. Pound, Phys. Rev. **95**, 8 (1954).
[71] V. M. Fain, UFN **64**, 273 (1958).
[72] Voskanyan, Klyshko, and Tusmanov, JETP **45**, 1399 (1963), Soviet Phys. JETP **18**, 967 (1964).
[73] R. H. Pantell and R. G. Smith, IEEE Trans. Microwave Theory and Techn. **11**, 317 (1963).
[74] V. M. Faĭn, Izv. vuzov (Radiofizika) **5**, 697 (1962).
[75] C. M. Kellington, Phys. Rev. Letts **9**, 57 (1962).
[76] Andresen, Welling, and Kellington, Phys. Rev. Letts **11**, 361 (1963).
[77] Franken, Hill, Peters, and Weinreich, Phys. Rev. Letts **7**, 118 (1961).
[78] P. A. Franken and J. F. Ward, Revs. Modern Phys. **35**, 23 (1963).
[79] N. Bloembergen, Proc. IEEE **51**, 124 (1963).
[80] A. Savage and R. C. Miller, Appl. Optics **1**, 661 (1962).
[81] Miller, Kleinman and Savage, Phys. Rev. Letts **11**, 146 (1963).
[82] Lax, Mavroides, and Edwards, Phys. Rev. Letts **8**, 166 (1962).
[83] Armstrong, Bloembergen, Ducuing, and Pershan, Phys. Rev. **127**, 1918 (1962).
[84] R. London, Proc. Phys. Soc. **80**, 952 (1962).
[85] P. L. Kelley, J. Phys. Chem. Solids, **24**, 607, 1113 (1963).
[86] D. A. Kleinman, Phys. Rev. **128**, 1761 (1962).
[87] V. I. Karpman, JETP **44**, 1307 (1963), Soviet Phys. JETP **17**, 882 (1963).
[88] L. N. Ovander, FTT **5**, 872 (1963), Soviet Phys.

Solid State 5, 641 (1963).
[89] N. Bloembergen and Y. R. Shen, Phys. Rev. A133, 37 (1964).
[90] J. F. Ward and P. A. Franken, Phys. Rev. A133, 183 (1964).
[91] V. L. Strizhevskii, FTT 6, 393 (1964), Soviet Phys. Solid State 6, 314 (1964).
[92] Hung Cheng and P. B. Miller, Phys. Rev. A134, 683 (1964).
[93] Terhune, Maker and Savage, Phys. Rev. Letts 8, 404 (1962).
[94] D. A. Kleinman, Phys. Rev. 126, 1977 (1962).
[95] R. C. Miller, Phys. Rev. 131, 95 (1963).
[96] Ashkin, Boyd, and Dziedzic, Phys. Rev. Letts 11, 14 (1963).
[97] Maker, Terhune, Nisenoff and Savage, Phys. Rev. Letts 8, 21 (1962).
[98] J. A. Giordmaine, Phys. Rev. Letts 8, 19 (1962).
[99] R. Terhune, Appl. Phys. Letts 2, 55 (1963).
[100] Akhmanov, Kovrigin, Khokhlov, and Chunaev, JETP 45, 1336 (1963), Soviet Phys. JETP 18, 919 (1964).
[101] J. K. Wright, Proc. IEEE 51, 1662 (1963).
[102] P. Franken, Proc. Third Quantum Electronics Conference, Paris, 1963, p. 1495.
[103] N. Bloembergen, Proc. Third Quantum Electronics Conference, Paris, 1963, p. 1501.
[104] Maker, Terhune, and Savage, Proc. Third Quantum Electronics Conference, Paris, 1963, p. 1559.
[105] Bass, Franken, Hill, Peters, and Weinreich, Phys. Rev. Letts 8, 18 (1962).
[106] R. C. Miller and A. Savage, Phys. Rev. 128, 2175 (1962).
[107] R. H. Kingston, Proc. IRE 50, 472 (1962).
[108] N. M. Kroll, Phys. Rev. 127, 1207 (1962).
[109] S. A. Akhmanov and R. V. Khokhlov, JETP 43, 351 (1962), Soviet Phys. JETP 16, 252 (1963).
[110] A. W. Smith and N. Braslau, J. Appl. Phys. 34, 2105 (1963).
[111] A. Javan and C. H. Townes, Quarterly Progress Report No. 66, MIT Research Lab. of Electronics, Cambridge, Mass., July 15, 1962.
[112] Dennis, Longaker, and Kingston, Proc. Third Quantum Electronics Conference, Paris, 1963, p. 1627.
[113] K. E. Niebuhr, Appl. Phys. Letts 2, 136 (1963).
[114] Bass, Franken, Ward, and Weinreich, Phys. Rev. Letts 9, 446 (1962).
[115] N. Bloembergen and P. S. Pershan, Phys. Rev. 128, 606 (1962).
[116] J. Ducuing and N. Bloembergen, Phys. Rev. Letts 10, 474 (1963).
[117] N. Bloembergen and J. Ducuing, Phys. Letts 6, 5 (1963).
[118] A. D. White, J. D. Ridgen, Proc. IRE 50, 1697 (1962).
[119] N. I. Adams and P. B. Schoefer, Appl. Phys. Letts 3, 19 (1963).
[120] Armstrong, Nathan, and Smith, Appl. Phys. Letts 3, 68 (1963).
[121] M. Garfinkel and W. E. Engeler, Appl. Phys. Letts 3, 178 (1963).
[122] S. P. S. Porto and D. L. Wood, J. Opt. Soc. Amer. 52, 251 (1962).
[123] B. P. Stoicheff, Proc. 10th Colloquium Spectroscopium Internationale, vol. 1, Spectran Books, Washington, 1963, p. 399.
[124] Danil'tseva, Zubov, Sushchinskiĭ, and Shuvalov, JETP 44, 2193 (1963), Soviet Phys. JETP 17, 1473 (1963).
[125] H. Kogelnik and S. P. S. Porto, J. Opt. Soc. Amer. 53, 1446 (1963).
[126] F. J. McClung and D. Weiner, J. Opt. Soc. Amer. 54, 641 (1964).
[127] E. E. Woodbury and W. K. Ng, Proc. IRE 50, 2367 (1962).
[128] Eckhardt, Hellwarth, McClung, Schwarz, Weiner, and Woodbury, Phys. Rev. Letts 9, 455 (1962).
[129] Geller, Bortfeld, and Sooy, Appl. Phys. Letts 3, 36 (1963).
[130] Geller, Bortfeld, Sooy, and Woodbury, Proc. IEEE 51, 1236 (1963).
[131] B. P. Stoicheff, Phys. Letts 7, 186 (1963).
[132] Zeiger, Tannenwald, Kern, and Herendeen, Phys. Rev. Letts 11, 419 (1963).
[133] Eckhardt, Borfeld, and Geller, Appl. Phys. Letts 3, 137 (1963).
[134] R. Chiao and B. P. Stoicheff, Phys. Rev. Letts 12, 290 (1964).
[135] Minck, Terhune, and Rado, Appl. Phys. Letts 3, 181 (1963).
[136] R. W. Hellwarth, Phys. Rev. 130, 1850 (1963).
[137] R. W. Hellwarth, Appl. Optics 2, 847 (1963).
[138] R. London, Proc. Phys. Soc. 82, 393 (1963).
[139] H. J. Zeiger and P. E. Tannenwald, Proc. Third Quantum Electronics Conference, Paris, 1963, p. 1589.
[140] Garmire, Pandarese, and Townes, Phys. Rev. Letts 11, 160 (1963).
[141] V. M. Faĭn and E. G. Yashchik, JETP 46, 695 (1964), Soviet Phys. JETP 19, 474 (1964).
[142] V. T. Platonenko and R. V. Khokhlov, JETP 46, 555 (1964), Soviet Phys. JETP 19, 378 (1964).
[143] G. Rivoire, Compt. rend. 258, 4001, 4470 (1964).
[144] E. Garmire, Bull. Amer. Phys. Soc. 9, 490 (1964).
[145] Hellwarth, McClung, Wagner, and Weiner, Bull. Amer. Phys. Soc. 9, 470 (1964).

Translated by J. G. Adashko